

1 **Structural and stratigraphic development of Offshore NW Sulawesi, Indonesia**

2

3 Herwin Tiranda<sup>1,2\*</sup>, Robert Hall<sup>2</sup>

4

5 1. Beicip-Franlab Asia, Suite 18-16, 18<sup>th</sup> Floor, G-Tower, 199 Jalan Tun Razak

6 50400 Kuala Lumpur, Malaysia

7 2. Southeast Asia Research Group, Royal Holloway University of London, Egham, Surrey, UK,

8 TW20 0EX

9

10 \*Corresponding author: Herwin Tiranda (herwin.tiranda@beicip.asia)

11

12 This paper is a non-peer reviewed preprint submitted to EarthArxiv.

13 **ABSTRACT**

14 The area of the Offshore NW Sulawesi lies between eastern Sundaland (Borneo) and the North Arm of  
15 Sulawesi. Possible influences on the basins include Paleogene rifting in the Celebes Sea and Makassar  
16 Strait, Neogene subsidence and uplift in Borneo, late Neogene subduction at the present-day North  
17 Sulawesi Trench, and displacements related to the Palu-Koro Fault. This study presents the results of  
18 structural and stratigraphic framework of the Offshore NW Sulawesi based on interpretation of 2D  
19 seismic surveys offshore and multibeam bathymetry. In this study, the Offshore NW Sulawesi region is  
20 divided into three parts: the Deepwater Tarakan Basin in the NW, the Muara Sub-basin in the west, and  
21 separated from these by the Palu-Koro Fault, the North Sulawesi Fold-Thrust Belt in the east. There is no  
22 continuation of the left-lateral strike-slip Palu-Koro Fault to the adjacent area of Borneo via the Muara  
23 Sub-basin and Deepwater Tarakan Basin. Both basins developed after extension began in the Middle  
24 Eocene associated with oceanic spreading in the Celebes Sea. Since then, sediment was fed to the basins  
25 from the east and south, with several episodes of subsidence, particularly during Early Miocene in the  
26 Muara Sub-basin. Rapid prograding shelves from eastern Borneo are linked to regional inversion and  
27 uplift on land since the Middle Miocene and led to gravity-driven movement in the Deepwater Tarakan  
28 Basin which formed toe-thrust faults in the latest Miocene. Deformation in the North Sulawesi Fold-  
29 Thrust Belt is interpreted to have occurred in the latest Miocene or Pliocene to present-day with  
30 subduction of Celebes Sea at the North Sulawesi Trench and movement on the Palu-Koro Fault.

31

32 **1 INTRODUCTION**

33 The region of Offshore NW Sulawesi between the North Arm of Sulawesi and Eastern Sundaland (Borneo)  
34 has been enigmatic in terms of the nature of the basin and structural development within the area. This  
35 area is located in a region where there is a transition between Eastern Sundaland which mainly consists  
36 of the continental basement and the Celebes Sea which is mainly oceanic crust (Hall, 2002, 2012; Weissel,  
37 1980). A large part of this area are lies within the complex North Sulawesi fold-thrust belt resulting from  
38 southward convergence of the Celebes Sea and underthrusting the North Arm of Sulawesi (Figure 1).

39

40 The study area is located within the Offshore NW Sulawesi (Figure 1) and is divided into 3 sub-areas. The  
41 North Sulawesi Fold-Thrust Belt is separated from the other 2 sub-areas in the west by the Palu-Koro  
42 Fault. The 2 sub-areas west of the Palu-Koro Fault which are closer to the Mangkalihat Peninsula of

43 Borneo have been identified as the part of NE Kalimantan Basin (Achmad and Samuel, 1984) or Tarakan  
44 Basin (PERTAMINA-BPPKA, 1996). The southern basin, which is also the main basin in the region, is  
45 named here as the Muara Sub-basin whereas the deeper part of the outer Tarakan Basin to the north of  
46 Muara Sub-basin is named the Deepwater Tarakan Basin. These 2 sub-areas are separated by a prominent  
47 structural high called the Maratua Ridge.

48

49 The Offshore NW Sulawesi area is almost completely unexplored. However, there are several exploration  
50 wells in the Muara Sub-basin (i.e. Karang Besar-1) and Deepwater Tarakan Basin (i.e. Aster-1, Tulip-1,  
51 Bougainville-1) with stratigraphic information but limited subsurface study. Moreover, the hydrocarbon  
52 exploration in this area during the 19<sup>th</sup> to 21<sup>st</sup> century mainly focused on the onshore parts of the Tarakan  
53 Basin and shallow water part of the basin. In the north of the study area, which lies within the Tarakan  
54 Basin is a well-known oil and gas province, and south of the Mangkalihat Peninsula is the Kutai Basin  
55 (Figure 1).

56

57 The nature of Offshore NW Sulawesi is still uncertain because the development of the basins is poorly  
58 understood, and their structural geometry is not obvious. There are two active subduction zones close to  
59 North Sulawesi: the Molucca Plate subducts to the west underneath the eastern part of the North Arm and  
60 there is subduction of the Celebes Sea under the central North Arm in a southward direction. All active  
61 volcanoes are in eastern North Sulawesi as a result of the Molucca Plate subduction. Recent geological  
62 mapping, GPS measurements and palaeomagnetic investigations show that this region has a very complex  
63 history including rapid movements and rotations possibly related to Neogene uplift, exhumation, and  
64 strike-slip deformation (Silver et al., 1983; Socquet et al., 2006; Surmont et al., 1994; Vigny et al., 2002).

65 The North Sulawesi Trench and Palu-Koro Fault formed around the Late Miocene to Pliocene (Advokaat,  
66 2015; Hall, 1996, 2002, 2012; Watkinson and Hall, 2016).

67

68 Further west, next to the Muara Sub-basin, the Maratua Ridge is the structural high parallel to the  
69 Maratua Fault Zone (Lentini and Darman, 1996; PERTAMINA-BPPKA, 1996). Several authors (Hidayati et  
70 al., 2007; Lentini and Darman, 1996; PERTAMINA-BPPKA, 1996) identified three sinistral wrench faults  
71 in the Tarakan Basin. The Semporna Fault in the northern part of Tarakan Basin is considered the  
72 northern wrench fault whereas Maratua Fault Zone in the south of the Tarakan Basin is a transpressional

73 fault zone interpreted to have formed the Maratua Ridge (Hidayati et al., 2007; Lentini and Darman, 1996;  
74 PERTAMINA-BPPKA, 1996). A boundary on the south side of the Muara Sub-basin closer to the coastline  
75 of the Mangkalihat Peninsula, has also been interpreted as a major wrench fault continuation of the left  
76 lateral Palu-Koro Fault in Sulawesi (Hidayati et al., 2007; Lentini and Darman, 1996; PERTAMINA-BPPKA,  
77 1996). The Muara Sub-basin is considered the transpressional zone formed by these two coupled shear  
78 zone (PERTAMINA-BPPKA, 1996). However, there is very limited field evidence of these wrench fault in  
79 the onshore area of the Tarakan Basin (PERTAMINA-BPPKA, 1996).

80

81 A number of plate reconstruction models have been proposed. Early Cenozoic rifting is marked by the  
82 separation of western Sulawesi from Borneo (Daly et al., 19991; Hall, 1996, 2002, 2012; Letouzey et al.,  
83 1990; Pieters et al., 1983) followed by subsidence during the Oligo-Miocene in Borneo (Hall, 2002, 2012).  
84 Significant uplift in Borneo has occurred from the Middle Miocene until the present day (Hall, 2002,  
85 2012). North Sulawesi Trench and Palu-Koro Fault formed later during the Late Miocene to Pliocene  
86 (Hall, 2002, 2012; Watkinson and Hall, 2016). Therefore, understanding the structural and stratigraphic  
87 development of Offshore NW Sulawesi is very important in evaluating prospectivity of the basins. This  
88 paper focuses on revealing the structural and stratigraphic development of Offshore NW Sulawesi based  
89 on 2D seismic reflection data and multibeam bathymetry map to get a better understanding of the basin  
90 history related to the regional tectonic history of the area so that potential petroleum systems can be  
91 identified and assessed.

92

## 93 **2 DATASET AND METHODOLOGY**

94 During 2005 to 2009, PGS acquired and processed 2D seismic datasets as a part of their EJMM  
95 MegaProject over offshore basins from East Java, Makassar, and Muara regions which provided  
96 significantly increased coverage and improved resolution. The area of interest is covered by a 2D seismic  
97 survey (Figure 2), which consists of 45 2D seismic lines (25 cross-lines trending NE-SW and 20 in-lines  
98 trending NW-SE). It was processed by PGS using Kirchhoff pre-stack time migration (PSTM) and covers  
99 an area of approximately 49,000 km<sup>2</sup>, with line spacing ranging from 12 km to 114 km. This also provides  
100 the dataset with a total length of approximately 3,940 km and extends to a depth of 9 seconds two way  
101 time (TWT).

102

103 High-resolution multibeam bathymetry was provided by GeoData Ventures (GDV) covering an area of  
104 approximately 65,000 km<sup>2</sup> of Offshore NW Sulawesi (Figure 2) and it was also incorporated in the study  
105 to see morphological features, sedimentary features, and active tectonic structures of Offshore NW  
106 Sulawesi. The multibeam bathymetry or Multibeam Echo-sounder Systems (MBES) record the images of  
107 seabed topography by measuring the time for a pulse to travel to the seabed and reflect to a receiver at  
108 the sea surface (Gafeira, 2010). Information about multibeam mapping and data processing which can  
109 measure sea floor depth to within a few centimeters using a high resolution echo sounder can be found in  
110 Orange et al. (2010). It has 25-15 m resolution and has been processed to a shaded-relief map by  
111 mimicking the effect generated by illumination at a low angle using Geographic Information System (GIS)  
112 software ArcMap 10.3.1 and ER Mapper. The shaded-relief map provides exceptional details of seafloor  
113 morphology, sedimentary features, and active geological structures as interpreted in Figure 3.

114

115 The methodology used in this paper is based on the recognition of seismic stratigraphy units and their  
116 stratal termination concepts (i.e. onlap, toplap, downlap, offlap, and truncations) according to Mitchum Jr  
117 et al. (1977). Time structure maps were built to understand the basin geometry, structural evolution, and  
118 sedimentary process at basin scale. Isochron maps which show relative sediment thickness are also  
119 provided to explain the basin geometry and evolution. The new work was integrated with pre-existing  
120 studies such stratigraphic records from published old wells within the study area (Atzeni and Guritno,  
121 2003; BP, 2000; PERTAMINA-BPPKA, 1996; Sunaryo et al., 1988; Wilson et al., 2007). Those data brought  
122 additional sedimentary and stratigraphic interpretations for Cenozoic units particularly in the Deepwater  
123 Tarakan Basin and Muara Sub-basin leading to a stratigraphic framework of Offshore NW Sulawesi.

124

### 125 **3 SEISMIC STRATIGRAPHY AND STRUCTURAL CHARACTERISTIC**

126 Seismic stratigraphy and structural characteristic of the study area are described in this chapter using  
127 three different sub-areas which are the Muara Sub-basin, Deepwater Tarakan Basin, and North Sulawesi  
128 Fold-Thrust Belt. Characteristics of seismic stratigraphy and structural development within these three  
129 subareas are described in this chapter. Each area developed with a different history of both structure and  
130 stratigraphy. Moreover, prominent structural highs and faults-bounding these three subareas make it  
131 complex to correlate between them as discussed below and summarized in Figure 4. Most of the  
132 interpretation has focused on the Muara Sub-basin and Deepwater Tarakan Basin where there is good

133 seismic coverage. The North Sulawesi Fold-Thrust Belt has significant differences from the Muara Sub-  
134 basin and Deepwater Tarakan Basin in structure and stratigraphy indicating a different tectonic history.  
135 An overview of composite seismic stratigraphy units across the three different sub-areas is summarized  
136 in Figure 4.

137

### 138 **3.1 Seismic stratigraphy of the Muara Sub-basin**

139 The Muara Sub-basin seismic stratigraphy has been divided into several seismic units based on seismic  
140 reflection characteristics, and major changes in seismic facies or unconformities marked by stratal  
141 terminations. Several wells with stratigraphic age control from published papers were used in this study  
142 and tied to the seismic packages particularly Karang Besar-1 well in the Muara Sub-basin (Sunaryo et al.,  
143 1988) and Makassar-A1 which is south of the Mangkalihat Peninsula (Camp et al., 2009) as shown in  
144 Figure 5. Based on stratigraphic information from the wells, the stratigraphy units in the Muara Sub-basin  
145 range in age from Eocene to Quaternary. There are eight main seismic units observed in the Muara Sub-  
146 basin which are, Unit X (Middle Eocene equivalent), Unit A (Upper Eocene equivalent), Unit B (Lower  
147 Oligocene equivalent), Unit C (Upper Oligocene equivalent), Unit D (Lower Miocene equivalent), Unit E  
148 (Middle Miocene equivalent), Unit F (Upper Miocene equivalent), and Unit G (Pliocene-Recent  
149 equivalent). The summary of seismic characteristics for each unit is shown on seismic line in Figure 6.

150

#### 151 **3.1.1 Unit X**

152 Unit X is characterized by variable amplitudes with discontinuous, chaotic reflections, and a low  
153 frequency seismic package (Figure 6). The internal seismic character of this unit is disrupted which  
154 makes it difficult to identify stratal terminations within it. In some of the seismic profiles, the top of this  
155 unit is marked by high amplitudes interpreted as a basal unconformity within this area. Several high  
156 amplitude reflections were observed as a localized feature within this unit which might indicate an  
157 acoustic basement or reflection multiples (Figure 7). This unit is also characterized by a series of faulted  
158 blocks with normal faults with planar surfaces cutting through it (Figure 7-Figure 9). However, the depth  
159 to which faults can be traced is not obvious.

160

161 The top of this unit is interpreted as Top Middle Eocene based on stratigraphic information from  
162 Makassar-A1 well in the southern part of Mangkalihat Peninsula according to Camp et al. (2009). The unit

163 is equivalent to the Middle Eocene Sembakung Formation and which include deformed volcanoclastics  
164 and Danau Formation basement rocks (Achmad and Samuel, 1984; Sunaryo et al., 1988). Possible  
165 siliciclastic facies of mixed shale and sandstone are mentioned by Achmad and Samuel (1984) and Wilson  
166 et al. (2007).

167

### 168 **3.1.2 Unit A**

169 Unit A is characterized by variable amplitudes, discontinuous and chaotic reflections, and a low frequency  
170 seismic package (Figure 6). In several seismic lines, this unit is characterized by continuous reflection  
171 with growth strata package terminating at a normal fault which indicates a syn-extensional unit (Figure  
172 9). This unit is deformed into a series of faulted blocks (Figure 7-Figure 9). The top of this unit is  
173 interpreted as Top Late Eocene based on stratigraphic control from Makassar-A1 well (Camp et al., 2009).  
174 According to Achmad and Samuel (1984) and Sunaryo et al. (1988), Unit A is an Upper Eocene marine  
175 siliciclastic facies with localized carbonate build ups.

176

### 177 **3.1.3 Unit B**

178 Unit B is characterized by high amplitudes, discontinuous and mounded reflections, mound geometry,  
179 and a low frequency (Figure 6). On several seismic profiles, this unit is observed as onlapping and  
180 downlapping on Unit A (Figure 7-Figure 9). The top of this unit is marked by high amplitude reflections  
181 which can be recognized easily within the study area as a regional carbonate unconformity equivalent to  
182 the Top Early Oligocene (Achmad and Samuel, 1984; Sunaryo et al., 1988). This unit is less deformed than  
183 Unit A and several internal reflection terminate at faults. Build ups and mounded features are the most  
184 common seismic reflection pattern (Figure 7-Figure 9). The unit is interpreted as a relatively shallow  
185 marine carbonates.

186

### 187 **3.1.4 Unit C**

188 Unit C has variable amplitudes with continuous and divergent reflections (Figure 6). This unit appears  
189 only in the Muara Sub-basin and is characterized by basin fill geometry with low frequency seismic  
190 reflections (Figure 7 and Figure 8). Several different stratal terminations are observed within this unit  
191 (e.g. toplap, downlap, and erosional truncation) as can be seen in Figure 7 and Figure 8. The top of this  
192 unit is interpreted as a local unconformity which is equivalent to the Top Late Oligocene based on

193 stratigraphic well control of Karang Besar-1 described by Sunaryo et al. (1988). This unit is equivalent to  
194 an Upper Oligocene unit which consists of siliciclastic facies or pelagic and hemipelagic mud. According to  
195 Achmad and Samuel (1984) and Sunaryo et al. (1988), the Upper Oligocene unit is dominated by  
196 calcareous mudstones of the Mangkabua Formation.

197

### 198 **3.1.5 Unit D**

199 Unit D is characterized by high amplitudes with continuous and divergent reflection (Figure 6). Most of  
200 the reflection patterns are sub-parallel. The basin shows basin fill geometry with high frequency  
201 reflections onlapping and downlapping towards Unit C (Figure 7 and Figure 8). The lower part of Unit D is  
202 characterized by chaotic and contorted reflections (Figure 8) interpreted as Mass Transport Complex  
203 (MTC). The top of this unit is interpreted as a local unconformity that is equivalent to the Top Early  
204 Miocene based on the Karang Besar-1 well described by Sunaryo et al. (1988). The depositional  
205 environment and lithology based on seismic stratigraphy is a shallow to a deep marine environment  
206 dominated by pelagic and hemipelagic mud. This unit is equivalent to the Lower Miocene Birang  
207 Formation of Achmad and Samuel (1984) and Sunaryo et al. (1988).

208

### 209 **3.1.6 Unit E**

210 Unit E has variable amplitudes with continuous and sigmoid reflections (Figure 6). The internal seismic  
211 pattern shows a progradation geometry downlapping towards Unit D. The high seismic frequency  
212 package is possibly dominated by siliciclastic facies of delta to pro delta facies. The top of this unit is  
213 interpreted as a local unconformity in the Muara Sub-basin that is equivalent to the Top Middle Miocene  
214 based on stratigraphic control from the Karang Besar-1 well described by Sunaryo et al. (1988). In several  
215 sections, particularly eastern edge of the Mangkalihat Peninsula, erosional truncation marks the  
216 boundary of Unit E and Unit F above shown in the interpreted seismic section of the SW part of MA08-04  
217 (Figure 9).

218

### 219 **3.1.7 Unit F**

220 Unit F has high amplitudes, continuous, and sigmoid reflections. The internal seismic pattern shows  
221 progradation geometry with a high frequency seismic package that downlaps towards Unit E (Figure 7-  
222 Figure 9). The top of this unit is equivalent to the Top Late Miocene according to the stratigraphic well



223 control from Karang Besar-1 described by Sunaryo et al. (1988). This unit is equivalent to the Upper  
224 Miocene Menubar Formation described by Achmad and Samuel (1984) and is a marine siliciclastic  
225 facies from a prograding delta shelf.

226

### 227 **3.1.8 Unit G**

228 Unit G is characterized by high amplitudes and continuous, and sigmoidal reflections (Figure 6). Internal  
229 reflections show as progradation geometry with high frequency downlapping towards Unit F (Figure 7-  
230 Figure 9). The top of this unit is the seabed. This unit is equivalent to the Pliocene-Recent according to  
231 stratigraphic well control in the Karang Besar-1 well illustrated by Sunaryo et al. (1988). It is mixed  
232 siliciclastic and carbonate facies from a prograding delta.

233

## 234 **3.2 Seismic stratigraphy of the Deepwater Tarakan Basin**

235 The Deepwater Tarakan Basin seismic sequence has been divided into several seismic packages.  
236 Stratigraphic control from one well (Bougainville-1) taken from published paper (Putra et al., 2018) and  
237 unpublished post-drill report (BP, 2000) was used to build the seismic stratigraphic framework in the  
238 basin (Figure 11). However, the Bougainville-1 well only reach the Upper Miocene stratigraphic unit as  
239 the total depth of the well. Thus, the age of seismic stratigraphy units older than Late Miocene was  
240 predicted in this paper (see section 4). Six seismic units have been identified within the Deepwater  
241 Tarakan Basin area which are, Unit X1, Unit C1, Unit D1, Unit E1, Unit F1, and Unit G1 (Figure 12).

242

### 243 **3.2.1 Unit X1**

244 Unit X1 has variable amplitudes, discontinuous and chaotic reflections, and low frequency (Figure 13-  
245 Figure 15). The top of this unit shows mounded geometry possibly related to an underlying volcanic  
246 edifice at an average depth of 9 secs TWT which can be easily traced within this area as a basal  
247 unconformity. The internal seismic pattern has localized high amplitudes with parallel reflections. This  
248 might be basaltic sills. The lithology of this unit is interpreted as oceanic crust with several local parallel  
249 basaltic sills.

250

251 **3.2.2 Unit C1**

252 Unit C1 is characterized by variable amplitudes with continuous and subparallel reflections. The  
253 reflection pattern of this unit becomes chaotic and contorted in the deformed zone of the Deepwater  
254 Tarakan Toe-Thrust (Figure 13-Figure 15). The low frequency seismic package downlaps towards Unit  
255 X1. The unit is interpreted as marine siliciclastic facies of pelagic mud and sandstone.

256

257 **3.2.3 Unit D1**

258 Unit D1 has variable amplitudes with parallel and subparallel reflections. The reflection pattern is partly  
259 continuous but becomes contorted in the Deepwater Tarakan Toe-Thrust (Figure 13-Figure 15). The  
260 seismic frequency is relatively low and reflection downlaps towards Unit C1. This unit is interpreted as  
261 marine turbidites with mixed siliciclastic facies.

262

263 **3.2.4 Unit E1**

264 Unit E1 is characterized by variable amplitudes with parallel reflections. The reflections are partly  
265 continuous and become contorted in the deformed zone of the Deepwater Tarakan Toe-Thrust (Figure  
266 13-Figure 15). The seismic frequency is relatively high. Stratal terminations at the base of the unit as it  
267 downlap on Unit D1. This unit is probably marine siliciclastic facies dominated by hemipelagic and pelagic  
268 mud.

269

270 **3.2.5 Unit F1**

271 Unit F1 is characterized by high amplitudes, parallel and continuous reflections, and high frequency  
272 (Figure 13-Figure 15). Although the reflections are slightly deformed and chaotic in the deformed zone of  
273 the Deepwater Tarakan Toe-Thrust, most of this unit has parallel and continuous reflections. This unit  
274 downlaps on Unit E1. The top of this unit is equivalent to the Late Miocene according to the stratigraphic  
275 well control from Bougainville-1 described by BP (2000). This unit is equivalent to the Upper Miocene  
276 Tabul and Santul Formations described by Achmad and Samuel (1984) which could be equivalent to the  
277 Upper Menubar Formation and is a marine siliciclastic prodelta facies from a prograding delta shelf.

278

279 **3.2.6 Unit G1**

280 Unit G1 is characterized by high amplitudes, parallel continuous reflections, and high frequency (Figure  
281 13-Figure 15). Internal features within this unit include, for example, local incisions infilled with  
282 sediment. This unit also shows growth strata packages on top of the Deepwater Tarakan Toe-Thrust with  
283 onlap onto Unit F1. The bottom part of Unit G1 downlaps on Unit F1, especially in the basinward section.  
284 According to the stratigraphic well control from Bougainville-1 (BP, 2000), the top unit is equivalent to  
285 the Top Pliocene-Recent which also pointed to the Tarakan and Bunyu Formations described by Achmad  
286 and Samuel (1984). The unit is marine shale facies with thin limestone beds of a prodelta environment  
287 (Achmad and Samuel, 1984).

288

289 **3.3 Seismic stratigraphy of the North Sulawesi Fold-Thrust Belt**

290 The North Sulawesi Fold-Thrust Belt seismic sequence has been divided into two main seismic units  
291 which are named the Lower Unit and Upper Unit. There is no stratigraphic well control within this area.  
292 The seismic stratigraphy is based on seismic reflection characteristics.

293

294 **3.3.1 Lower Unit**

295 The Lower Unit is characterized by variable amplitudes with parallel and chaotic reflections, and low  
296 frequency (Figure 17-Figure 18). The most obvious feature of this unit is a highly deformed character that  
297 is related to a fold-thrust belt. Several erosional truncations are observed within this unit. Possible  
298 lithologies for this unit include mixed basement and cover rocks with volcanoclastic-siliciclastic facies.

299

300 **3.3.2 Upper Unit**

301 The Upper Unit is characterized by variable amplitudes with parallel reflections and high frequency  
302 seismic reflections (Figure 17-Figure 18). Growth strata are obvious from reflection patterns in this unit.  
303 The lower part shows stratal termination on the Lower Unit (e.g. downlap and onlap). The unit is  
304 interpreted as a marine pelagic and hemipelagic mud dominated facies.

305

306 **3.4 Structural observations and results**

307 **3.4.1 Muara Sub-basin**

308 Several different tectonic phases can be recognized from structures of the Muara Sub-basin. In the Muara  
309 Sub-basin, the oldest structures are below the basal unconformity in Unit X and are interpreted as the  
310 result of pre-Eocene folding and thrusting. Then there was a phase of uplift and erosion to produce the  
311 basal unconformity. The extensional phase which initiated rifting is identified from faults seen on seismic  
312 lines (Figure 7-Figure 9), followed by deposition of Unit A (Upper Eocene). The phase of extension was  
313 inactive later and is interpreted as the end of rifting followed by the break-up unconformity in the Muara  
314 Sub-basin. Unit B was then deposited unconformably on top of Unit A (Figure 7-Figure 9).

315

316 However, there was some reactivation of normal faulting seen on seismic lines which cut through Unit B  
317 (Figure 7-Figure 9) and normal faulting seems to continue into the younger unit. But during the  
318 deposition of Unit C, Unit D, Unit E, Unit F, and Unit G almost no significant normal faulting is observed on  
319 seismic lines as shown on the time structure map (Figure 10). Unit C infilled locally in the Muara Sub-  
320 basin during the Late Oligocene (Figure 10). Thick sediment of Unit D is interpreted as the result of rapid  
321 subsidence and sedimentation during the Early Miocene (Figure 7 and Figure 8).

322

323 Inversion and uplift caused Unit E to prograde to the NE during the Middle Miocene. Inversion of normal  
324 faults is interpreted to have caused major uplift in the Mangkalihat High and adjacent area which  
325 contributed sediment to the Muara Sub-basin. The inverted normal faults are basement-involved  
326 structures and affected all units as observed on seismic (Figure 9). During the period of inversion, Unit F  
327 (Upper Miocene) and Unit G (Pliocene-Recent) were deposited in the Muara Sub-basin. Inversion seems  
328 to continue to the present day as seismic reflections of Unit G show erosional truncation at the seabed  
329 (Figure 9).

330

331 **3.4.2 Deepwater Tarakan Basin**

332 The Deepwater Tarakan Basin is dominated by a fold-thrust belt which is characterized by an imbricated  
333 fault-propagation fold system (Figure 13-Figure 15). In the contractional deformation province, the  
334 sequence of thrusting tends to younger basinward. This is interpreted as a gravity-driven structure as  
335 observed in several seismic lines (Figure 15). Unit X1 is a relatively undeformed unit with morphology

336 features that are interpreted as a volcanic edifice forming part of the Eocene oceanic basement (Figure 13  
337 and Figure 14). Unit C1, Unit D1, Unit E1, and Unit F1 observed on seismic are interpreted as the  
338 depositional stage during the Late Eocene to Late Miocene in the Deepwater Tarakan Basin.

339

340 The timing of the development of toe-thrust faulting in the Deepwater Tarakan Basin is interpreted to  
341 have occurred in the Latest Miocene or Pliocene, post-deposition of Unit F1. Seismic lines show the unit  
342 above F1 is lying unconformably on top of Unit F1 as syn-kinematic and post kinematic units (Figure 13-  
343 Figure 15). The regional detachment level of this toe-thrust fault is interpreted to be in Unit C1 (Upper  
344 Eocene to Oligocene) and is suggested to have been triggered by a gravity-driven mechanism (Figure 15  
345 and Figure 16). Little deformation above Unit F1 was developed in the latest stage of fold-thrust belt  
346 formation as syn-kinematic units.

347

348 Furthermore, observation from multibeam bathymetry shows that the toe-thrust is not visible on the  
349 seabed (Figure 3) which implies the uppermost of Unit G1 represents the post-kinematic units. However,  
350 based on the seismic interpretation, the growth strata on top of Unit F1 indicates that the faulting may  
351 have been active during the earlier stages of deposition of Unit G1 (Figure 13 and Figure 14).

352

### 353 **3.4.3 North Sulawesi Fold-Thrust Belt**

354 The North Sulawesi Fold-Thrust Belt has a complex structure (Figure 17). The northern edge of this area  
355 is bounded by the North Sulawesi Trench which is interpreted as the frontal thrust system of the North  
356 Sulawesi Fold-Thrust Belt. It has a different character compared to the fold-thrust belt in the Deepwater  
357 Tarakan Basin. Most of the thrust faults dip south and folds have a symmetrical geometry. It is not clear  
358 which is the detachment level due to poor seismic imaging in the deeper section with chaotic reflections  
359 (Figure 17). However, two trends in the fold-thrust belt are observed within this area which are NE-SW  
360 and ENE-WSW (Figure 3).

361

362 There is no well control and therefore when deformation began is unknown. Seismic observations show  
363 the Lower Unit is deformed (Figure 17 and Figure 18). Subsequently, sediment of Upper Unit is  
364 interpreted to have been derived from the south of the North Sulawesi Fold-Thrust Belt, and covered the  
365 deformed Lower Unit. Development of the fold-thrust belt seems to continue to the present day as

366 observed on seismic since the Upper Unit is also deformed by folds and thrust faults (Figure 17 and  
367 Figure 18). Multibeam bathymetry supports this interpretation. Interpretation suggests the development  
368 of extensional basin in the southernmost part of the North Sulawesi Fold-Thrust Belt was the response to  
369 development of NE-SW trending thrust faults and ENE-WSW trending thrust faults further north (Figure  
370 3 and Figure 19). Based on observations on land the deformation probably occurred during the Pliocene to  
371 Recent.

372

## 373 **4 DISCUSSION**

### 374 **4.1 Age of the basin units**

#### 375 **4.1.1 Unit X1**

376 The oldest part of the Celebes Sea is underlain by basaltic basement according to Silver and Rangin  
377 (1991) and, based on the studies of the geochemistry from the two holes drilled in the Celebes Sea during  
378 ODP Leg 124, has a Mid-Oceanic Ridge Basalt (MORB) affinity. The age of the Celebes Sea crust, based on  
379 magnetic anomalies immediately east of the Deepwater Tarakan Basin, is Eocene (Weissel, 1980). This is  
380 supported by overlying pelagic sediments which contain radiolarians of Middle Eocene age (Nichols and  
381 Hall, 1999; Rangin et al., 1990) and by seismic refraction measurements (Murauchi et al., 1973).

382

383 The basal unconformity at the top of Unit X1 in the Deepwater Tarakan Basin shows generally almost flat  
384 geometry with a local cone-shaped structure which may indicate carbonate build up or volcanic structure  
385 (Figure 13-Figure 15). The latter is much more likely since no aggradation patterns of carbonate builds up  
386 were encountered in this unit from the seismic profile. These features are now at an average depth of 7.5  
387 seconds (TWT). Average abyssal water depths in the Celebes Sea are approximately 5 km depth based on  
388 the age-depth relationship proposed by Chung-Hwa et al. (1990). Moreover, the interpreted volcanic  
389 edifices in the Deepwater Tarakan Basin are up to than 1 km across which is consistent with typical  
390 basaltic volcanoes. We propose the Unit X1 is equivalent to the Middle Eocene basaltic basement in the  
391 Celebes Sea.

392

#### 393 **4.1.2 Units C1, D1, E1**

394 The contact of Unit C1 and Unit X1 is unconformable over most of the Deepwater Tarakan Basin. Unit C1  
395 has well-stratified reflections which are almost continuous with variable amplitudes and dominate in the

396 unit. Similar seismic reflection patterns also observed in the Unit D1, Unit E1, Unit F1, and Unit G1 in the  
397 Deepwater Tarakan Basin. The reflections may indicate mixed pelagic hemipelagic mud with minor  
398 coarse-grained siliciclastic facies. Some local chaotic reflections are interpreted as Mass-Transport  
399 Complexes (MTC) of deep marine turbidites, particularly at the base of Unit C1. The sedimentological  
400 record in the easternmost Celebes Sea indicates pelagic to hemipelagic mudstone dominated almost the  
401 entire section above the Eocene basaltic basement (Nichols and Hall, 1999).

402

403 Middle-Upper Miocene quartz rich turbidite sandstones are discussed by Nichols and Hall (1999). The  
404 provenance of the quartz rich sandstones indicates these turbidites were derived from erosion of  
405 continental crust (Nichols and Hall, 1999). Plate tectonic reconstructions of the Celebes Sea region which  
406 is bordered by Borneo in the west, suggest no relative motion between the Deepwater Tarakan Basin and  
407 present-day adjacent areas (Hall, 1996, 2002, 2011, 2012). This implies that sediment influx during the  
408 Middle-Late Miocene, as suggested by Nichols and Hall (1999), came from Borneo. Hamilton (1979) also  
409 supports the idea that sediments were likely derived from Borneo to the Celebes Sea.

410

411 Nichols and Hall (1999) suggested that during the Middle-Late Miocene drainage systems were well-  
412 developed with large sediment supply of continentally-derived material. This channel system may have  
413 allowed the sediments supply to flow downslope from landward of Borneo to the Celebes Sea through the  
414 Deepwater Tarakan Basin. Multibeam bathymetry also shows a similar well-developed channel pattern  
415 which flows to the Deepwater Tarakan Basin (Figure 3). A further observation from the seismic profile  
416 also implies the vertical stacking channel system on the younger units above Unit X1 that broadly has  
417 NW-SE trend. Based on this, we suggest that the units above Unit X1 were derived from Borneo and  
418 equivalent in age to Cenozoic sediments of the Tarakan Basin described by previous authors (Achmad  
419 and Samuel, 1984; BP, 2000; PERTAMINA-BPPKA, 1996).

420

421 Here, we consider Unit C1 is equivalent to Upper Eocene to Oligocene Sujau Formation and Mangkabua  
422 Formation of the Tarakan Basin (Achmad and Samuel, 1984; PERTAMINA-BPPKA, 1996). Unit D1 is  
423 equivalent to the Lower Miocene Naintupo Formation whereas Unit E1 is equivalent to the Middle  
424 Miocene Tabul Formation (Achmad and Samuel, 1984; PERTAMINA-BPPKA, 1996).

425

426 **4.1.3 Lower Unit and Upper Unit**

427 As described in the previous chapter, the Lower Unit and Upper Unit of The North Sulawesi Fold-Thrust  
428 Belt has different internal seismic reflection pattern. The older unit, Lower Unit, has variable continuity of  
429 reflection where mostly are chaotic and deformed while Upper Unit mostly characterized by growth  
430 strata package with continuous, high amplitude, and high frequency that lying unconformably the Lower  
431 Unit. The development of the North Sulawesi Fold-Thrust Belt may contribute to the different  
432 sedimentological record in this region as represented by reflection pattern for each unit.

433

434 Possible Pre-Pliocene sediments derived from Borneo to the North Sulawesi Fold-Thrust Belt are quite  
435 plausible since the North Sulawesi Fold-Thrust Belt or what Djajadihardja et al. (2004) called as North  
436 Sulawesi Accretionary Prism formed during the Latest Miocene or Pliocene which developed by North  
437 Sulawesi Trench (Hall, 1996, 2012; Rudyawan, 2016). Lower Unit is much likely equivalent with a Pre-  
438 Pliocene unit, similar to those in the Celebes Sea and Deepwater Tarakan Basin.

439

440 During the period of the North Sulawesi Trench was developing, Nichols and Hall (1999) suggested that  
441 this trench acted as a traps sediment supplied from clastic material transported from Borneo. Possible  
442 sediment source to the North Sulawesi Fold-Thrust Belt is from the North Arm of Sulawesi. In this case,  
443 Upper Unit is much likely equivalent with Pliocene-Recent unit of the North Arm of Sulawesi.

444

445 **4.2 Nature of the basins**

446 **4.2.1 Muara Sub-basin**

447 The Muara Sub-basin was developed since the initiation of the extensional event during Middle Eocene  
448 which corresponds to the rifting in the Celebes Sea. It has a broadly NNW-SSE trend of normal fault which  
449 continue until Late Eocene. During Oligocene, no significant tectonic activity in the Muara Sub-basin and  
450 the adjacent area. Thermal subsidence is suggested caused the basin to subside which marked by thick  
451 Early Miocene sediment deposited on top the Oligocene unit. Significant inversion since Middle Miocene  
452 caused the uplifting in the Mangkalihat Peninsula and prograding shelf to the Muara Sub-basin.

453

454 Muara Sub-basin and the Deepwater Tarakan Basin is separated by NW-SE trending Maratua Ridge as a  
455 structural high. We see no evidence to support the suggestion of Hidayati et al. (2007); Lentini and



456 Darman (1996); PERTAMINA-BPPKA (1996) that Maratua Ridge is the transpressional wrench fault  
457 bounded the Muara Sub-basin and Deepwater Tarakan Basin in the north. A further observation from the  
458 seismic and multibeam bathymetry indicates no continuation of Palu-Koro Fault to the eastern part of  
459 Borneo (Mangkalihat Peninsula, Muara Sub-basin, and Deepwater Tarakan Basin). However, in the  
460 deeper section of the seismic profile immediately north of the Muara Sub-basin, there is a minor pop-up  
461 structure developed in relatively very young units (possibly very recent structure) as shown in **Error!**  
462 **Reference source not found.** But, it does not necessarily mean Maratua Ridge is the transpressional  
463 wrench fault. Moreover, this structure not affecting the Maratua Ridge it self, contradictive with Hidayati  
464 et al. (2007) suggestion.

465  
466 Maratua Ridge seems to be an older structure which formed in the Eocene as transform fault and related  
467 to the formation of Eocene spreading in the Celebes Sea which no longer active since Oligocene (R. Hall,  
468 pers. comm. 2017). Interpretation from Fraser et al. (2003) based on the gravity lineament trend of North  
469 Makassar Straits indicates NW-SE trending structure in the Mangkalihat Peninsula and Maratua Ridge.  
470 However, Fraser et al. (2003) interpreted this lineament as structural freeways that formed  
471 transpressional fault of Maratua Faut Zone and Sangkulirang Fault Zone as a continuation of Palu-Koro  
472 Fault. Again, no evidence from the seismic and multibeam bathymetry to support the suggestion from  
473 Fraser et al. (2003) that Palu-Koro Fault extends towards the Mangkalihat Peninsula and Maratua Ridge.

474

#### 475 **4.2.2 Deepwater Tarakan Basin**

476 The Deepwater Tarakan Basin exhibit well-developed gravity tectonics related structural provinces with  
477 extensional and contractional deformation provinces. The contractional deformation provinces are  
478 characterized by a toe-thrust fault, whilst the extensional deformation provinces are characterized by  
479 detached extensional fault. The transitional zone separating the contractional deformation provinces  
480 from extensional deformation provinces. The gravity tectonics in the Deepwater Tarakan Basin is  
481 interpreted to have occurred in the Mid-Late Miocene (Hidayati et al., 2007) whereas, recent study from  
482 Putra et al. (2018) indicates the deformation of Deepwater Tarakan Basin took place in the late of Early  
483 Miocene detaching in the thick shale of Lower Miocene stratigraphy unit which still active until present  
484 day. In the transitional zone, shale diapirs or mud pipes can be developed (Morley et al., 2011) as can be  
485 seen from Putra et al. (2018) interpretation in the Deepwater Tarakan Basin.

486

487 No evidence to support the suggestion of deformation timing and detachment level based on Hidayati et  
488 al. (2007) and Putra et al. (2018). Instead, based on our multibeam and seismic observation, the  
489 Deepwater Tarakan Basin toe-thrust probably developed in the Latest Miocene or Pliocene post-  
490 deposition of Unit F1. It has major NNE-SSW thrust fault which triggered by the gravity driven  
491 mechanism caused by major NNE-SSW extensional faulting in the western part of it due to the loading of  
492 progradation of large delta system to the east. The uplift onshore since Middle Miocene also possibly  
493 controlled to the slope development of the Deepwater Tarakan Basin fold-thrust belt detachment.  
494 Moreover, the down-flexing of subducting Celebes Sea slab in the latest Miocene or Pliocene might also  
495 allowed gravitational sliding to the Deepwater Tarakan Basin. The thick shale detachment in the  
496 Deepwater Tarakan Basin is very unlikely, since seismic observation denotes relatively thin layer possible  
497 shale detachment unit above basal unconformity. The deformation of Deepwater Tarakan Basin is most  
498 likely inactive since Pleistocene as seen from seismic and multibeam bathymetry that no well-developed  
499 fold-thrust belt in the seabed, contrast with Putra et al. (2018) suggestion that the toe-thrust fault  
500 development still active in the present.

501

502 The rate of sedimentation (V-Sed) model based on Hidayati et al. (2007) shows high sedimentation rate in  
503 the contractional deformation provinces in the Latest Miocene and reaches approximately 300-400m/my,  
504 coincides with the onset of toe-thrust fault development. In contrast, the rate of sedimentation during  
505 Latest Miocene in the extensional deformation provinces reaches approximately 150-200m/my (Hidayati  
506 et al., 2007). This has triggered the overpressure generating mechanism caused by disequilibrium  
507 compaction due to rapid sedimentation in the contractional deformation province in Miocene (Putra et  
508 al., 2018). As a consequences, deformation along a shale detachment will tend to cause dewatering and  
509 loss of the initial shale weaknesses, which might not cause reactivation of the initial detachment during  
510 the new deltaic cycle or new uplift event onshore (Morley et al., 2011). This might one of the many  
511 reasons why the deformation of Deepwater Tarakan Basin toe-thrust fault is inactive since Pleistocene to  
512 present-day.

513

514 Hidayati et al. (2007) also suggested there was a significant dropped of sedimentation rate from Latest  
515 Miocene to Recent in the contractional deformation provinces (-150m/my) whereas in the extensional

516 deformation provinces the sedimentation rate was increased (+330m/my). Growth faulting in the  
517 extensional deformation provinces possibly developed huge accommodation space during Late Miocene  
518 deformation while large amount of sediments were transported far to the basinward and were  
519 accommodated by the development of toe-thrust fault in the contractional deformation provinces. During  
520 the next cycle of deltaic sedimentation, the extensional domain was filled up with large amount Pliocene to  
521 Recent sediments with only few amount of sediments was deposited in the basinward (contractional  
522 domain). The bulk of Pliocene to Recent sediments probably was trapped in the extensional deformation  
523 provinces (Hidayati et al., 2007), implies no triggering mechanisms to further reactivate the toe-thrust  
524 fault or even to develop new fault.

525

#### 526 **4.2.3 North Sulawesi Fold-Thrust Belt**

527 Development of the North Sulawesi Fold-Thrust Belt is related to the initiation of North Sulawesi Trench  
528 which formed in the latest Miocene or Pliocene (Hall, 1996, 2012; Rudyawan, 2016). The development of  
529 the North Sulawesi Fold-Thrust Belt was suggested by Djajadihardja et al. (2004) to have formed at 5 Ma  
530 as the subduction began.

531

532 Observation from the multibeam and bathymetry shows a change of major structural trend in the North  
533 Sulawesi Fold-Thrust Belt from broadly NE-SW in the southern part, to ENE-WSW fold-thrust belt trend  
534 in the north. This indicates different phases of structural development in the North Sulawesi Fold-Thrust  
535 Belt. Djajadihardja et al. (2004) indicate that clockwise rotation of the North Arm of Sulawesi along the  
536 Palu-Koro Fault caused the change in trend of the fold-thrust belt from NE-SW to ENE-WSW trend. This  
537 idea is also supported by the model postulated by Advokaat (2015).

538

539 A further observation from the seismic across North Sulawesi Fold-Thrust Belt also indicates the  
540 development of extensional basin and rapid subsidence in the offshore North Arm of Sulawesi. This  
541 indication possibly related to the rollback of the southward subducting Celebes Sea since the Pliocene  
542 (Advokaat, 2015; Advokaat et al., 2017). Young extension in the North Arm of Sulawesi occurred between  
543 8.5 Ma and 4.4 Ma (Advokaat, 2015) which might relate to the extensional event in a southern offshore of  
544 the North Sulawesi Fold-Thrust Belt.

545

546 The Palu-Koro Fault formed relatively recently during the Pliocene (5 Ma) based on the non-coaxial strain  
547 in the Palu metamorphic rocks (Watkinson, 2011). Furthermore, the northward rollback of the  
548 southward subducting Celebes Sea slab which also created the North Sulawesi Trench may have been  
549 mechanically linked to the Palu-Koro Fault (Govers and Wortel, 2005; Silver et al., 1983; Vigny et al.,  
550 2002) as a subduction-transform edge propagator (STEP) fault (Govers and Wortel, 2005). Walpersdorf  
551 et al. (1998) and Bellier et al. (2006) suggested the instantaneous motions by GPS estimated the long  
552 term rates based on the interpretation of the slip rate of Palu Koro Fault and the Pliocene rotation. This  
553 suggestion is also supported by the observation from multibeam bathymetry and seismic reflection in the  
554 North Sulawesi Fold-Thrust Belt that the deformation is still ongoing at the present day.

555

### 556 **4.3 Structural and stratigraphic evolution**

557 A new structural and stratigraphic evolution model of the Offshore NW Sulawesi is proposed to give an  
558 insight into the development of the basins. Schematic summary of interpreted basin evolution model is  
559 shown in Figure 20 and Figure 21. The synoptic model is based on observations and interpretation of  
560 seismic data and multibeam bathymetry. A literature review was used to provide the regional tectonic  
561 context for Offshore NW Sulawesi and adjacent area. Six major stages of structural and stratigraphic  
562 evolution from Middle Eocene to present day are recorded in the Offshore NW Sulawesi, as described  
563 below.

564

#### 565 **4.3.1 Middle Eocene – Late Eocene stage**

566 In eastern Borneo and adjacent areas, extension began in the Middle Eocene (Hall, 2002, 2012) which led  
567 to the formation of oceanic crust in the Celebes Sea (Weissel, 1980). The extension phase extended  
568 towards the Makassar Strait which initiated the Eocene rifting separating West Sulawesi from Borneo  
569 (Hall, 2002, 2012). Extension is also observed in the Muara Sub-basin where rifting initiated in this area  
570 at the same time. During this time, the Maratua Ridge acted as a transform fault until the Celebes Sea  
571 ceased to spread.

572

573 Top Unit X1 represents the basal unconformity above oceanic crust that developed after the cessation of  
574 rifting in the Celebes Sea. In the Deepwater Tarakan Basin, minor structuration developed during Middle  
575 Eocene time. Most of the rifting features are observed immediately west of it, in the Tarakan Basin

576 (Lentini and Darman, 1996; Satyana et al., 1999). The basement fabric in the Muara Sub-basin, Top Unit X,  
577 shows major NW-SE trending faults which are similar to basement lineaments in the Makassar Straits  
578 (Hall et al., 2009; Nur'Aini et al., 2005). Similar features are also observed in the other parts of eastern  
579 Borneo in the Kutai Basin (Cloke et al., 1999a; Cloke et al., 1999b) and Tarakan Basin (Lentini and  
580 Darman, 1996; Satyana et al., 1999).

581

582 During the Late Eocene, the channel-like structures trending NW-SE of the Top Unit X1 in the Deepwater  
583 Tarakan Basin seems to have accommodated Unit C1 which was transported from the west to the basin.  
584 The depositional environment is interpreted as deep marine with mixed bathyal shales and fine  
585 interbedded siliciclastics. Late Eocene radiolarian pelagic and hemipelagic mud which indicates deep  
586 marine environment were also found in the Celebes Sea (Nichols and Hall, 1999) which is closer to the  
587 Deepwater Tarakan Basin. In the Muara Sub-basin, rifting in the Middle Eocene accommodated Unit A  
588 which is interpreted as mixed bathyal shales and fine interbedded siliciclastics transported to the basin  
589 from southwest which in the landward direction is dominated by marginal marine coals and siliciclastics  
590 (Wilson and Evans, 2002).

591

#### 592 **4.3.2 Early Oligocene – Late Oligocene stage**

593 In the Oligocene, there was a deep marine area to the east of Borneo (Hall, 2002). During this period  
594 there was no significant tectonic activity in the Muara Sub-basin and Deepwater Tarakan Basin. The  
595 Muara Sub-basin and the adjacent area was mostly dominated by widespread carbonate build ups  
596 (Achmad and Samuel, 1984; Sunaryo et al., 1988; Wilson and Evans, 2002). Unit B, which is interpreted as  
597 carbonate, was unconformably deposited on Unit A. The contact of Unit A and Unit B is interpreted as the  
598 breakup unconformity. Deposition continued until the Late Oligocene, and in the Muara Sub-basin Unit C  
599 fills the basinal area which was surrounded by carbonate builds up of Early Oligocene age.

600

601 The Deepwater Tarakan Basin was a deep marine environment. Little sediment was shed to the east of  
602 Borneo during the Oligocene (Hall, 2002). There was no significant change in the sediment source in the  
603 Deepwater Tarakan Basin. During this period, Unit C1 is interpreted as transported into the Deepwater  
604 Tarakan Basin from the west. Unit C1 is interpreted as a basinal area east of a prograding shelf where  
605 bathyal shales and fine interbedded siliciclastics were deposited.

606

607 **4.3.3 Early Miocene stage**

608 The Early Miocene was marked by a change of sedimentation character in Borneo (Hall, 2002). A large  
609 amount of clastic sediments eroded from Central Borneo fed eastern Borneo particularly the Kutai Basin  
610 initiating a prograding delta to the east (Hall, 2002). In the Muara Sub-basin, thermal subsidence caused  
611 the basin to subside rapidly following the deposition of thick mixed siliciclastic facies of Unit D. Most of  
612 the seismic lines show parallel continuous reflections resting on top of Unit C. During this period, there  
613 was a significant change of depositional environment from relatively shallow water to a deep-water  
614 environment.

615

616 Observation of Unit D from seismic indicates contorted and chaotic reflections of a Mass Transport  
617 Complex (MTC) passing up into more parallel and continuous reflections of pelagic and hemipelagic mud  
618 dominated sediments. Unit D is interpreted as bathyal mixed fine grained siliciclastics. In the Tarakan  
619 Basin, the large amount of sediment contributed to the development of a delta system prograding  
620 eastward to the Deepwater Tarakan Basin. During this period, the Deepwater Tarakan Basin is  
621 interpreted as a deep marine setting with mixed siliciclastic facies of Unit D1 resting on top of Unit C1.

622

623 **4.3.4 Middle Miocene stage**

624 In the Middle Miocene, inversion and uplift caused rapid clastic deltaic deposition in the Tarakan Basin  
625 (Satyana et al., 1999). However, several authors suggested the inversion began in the Early Miocene  
626 particularly in the Kutai Basin and fed sediment to the Mahakam Delta (Chambers and Daley, 1997).  
627 Observations from seismic in the offshore area of eastern and southern part of Mangkalihat Peninsula  
628 suggest Middle Miocene inversion and uplift.

629

630 Inversion and uplift in the Mangkalihat Peninsula and adjacent areas also caused prograding deltaic  
631 deposition in the Muara Sub-basin. This is indicated by deposition of Unit E interpreted as a delta  
632 prograding to the basinal area in the north. Similarly, in the Deepwater Tarakan Basin, the deltaic system  
633 of the Tarakan Basin seems to have prograded to the basinal area. This caused the deposition of Unit E1  
634 which is interpreted as bathyal shales and fine interbedded siliciclastics.

635

636 **4.3.5 Late Miocene stage**

637 During the Late Miocene, inversion and uplifting seem to have continued. This is indicated from several  
638 seismic sections observed offshore east of Mangkalihat Peninsula which show inverted normal faults. An  
639 erosional unconformity and other stratal terminations show evidence of continuation of inversion in the  
640 Late Miocene.

641

642 As a result, Unit F, which is interpreted as mixed carbonates and siliciclastics, prograded into the Muara  
643 Sub-basin and was deposited on top of Unit E. Similarly, in the Tarakan Basin, during the Late Miocene,  
644 rapid clastic deposition from landward to the basin caused loading of the prograding delta which is  
645 represented by Unit F1. Consequently, normal faulting in the shelf caused gravity driven movements to  
646 the Deepwater Tarakan Basin and formed toe-thrust faults in the Latest Miocene. This gravity driven  
647 structure is interpreted as detaching on Unit C1 which is dominated by shales.

648

649 Deformation in the North Sulawesi Fold-Thrust Belt associated with the southward subducting Celebes  
650 Sea is interpreted to have occurred since the Latest Miocene or Early Pliocene post deposition of Lower  
651 Unit during this stage. Deformation of North Sulawesi Fold-Thrust Belt followed by loading of the eastern  
652 edge of the Muara Sub-basin and Mangkalihat areas probably caused subsidence of the carbonate features  
653 observed offshore east of the Mangkalihat peninsula. Onset of deformation in the North Sulawesi Fold-  
654 Thrust Belt might also has contributed to the loading and clockwise tilting of Celebes Sea, created east  
655 dipping detachment ramp that allows gravity driven movements and sediment routing systems to the  
656 Deepwater Tarakan Basin.

657

658 **4.3.6 Pliocene – present-day stage**

659 Inversion and uplift in Borneo are interpreted to have continued from the Middle Miocene until the  
660 present day as observed from several seismic lines. This caused progradation of the shelf which  
661 developed during the Pliocene to Recent in both Muara Sub-basin and Deepwater Tarakan Basin.

662

663 In the Muara Sub-basin, Unit G was deposited on top of Unit F as a prograding shelf of mixed carbonate  
664 and siliciclastic facies. In contrast, in the Deepwater Tarakan Basin, there were significant decrease of  
665 sedimentation rate to the more basinal setting in the east. During this phase clastic deposition of Unit G1

666 caused progradation to the more basinal setting in the east. Development of toe-thrust faulting in the  
667 Deepwater Tarakan Basin is most likely inactive since the Pleistocene as observed from seismic where  
668 uppermost strata of Unit G1 (Pleistocene-Recent eq. Units) onlap lowermost Unit G1 (Pliocene eq. Units;  
669 Figure). Observations from multibeam bathymetry also indicates no well-developed toe-thrust faults at  
670 the seabed in the present-day.

671

672 Ongoing deformation in North Sulawesi Fold-Thrust Belt which is associated with the subducting Celebes  
673 Sea since latest Miocene has a significant impact on the structural and stratigraphic development. The  
674 Upper Unit was transported offshore from North Arm of Sulawesi and was unconformably overlies the  
675 Lower Unit. During this stage, rollback of North Sulawesi Trench has caused different structural  
676 development in the North Sulawesi Fold-Thrust Belt. Since Pliocene, the Palu Koro Fault was  
677 mechanically linked to the North Sulawesi Trench. The pattern of fold-thrust belt has rotated clockwise  
678 and moved towards the north to its present-day position, whereas immediately north of North Arm of  
679 Sulawesi in the offshore extension and subsidence were well developed, followed by deposition of Upper  
680 Unit.

681

## 682 **5 HYDROCARBON IMPLICATIONS**

683 The basin development and evolution have significant implications for the hydrocarbon prospects within  
684 the basins. Thus, the structural and stratigraphic evolution model gives an insight into the basin  
685 development and petroleum assessment in the basins. Moreover, assessing the basins based on the  
686 sediment thickness map using isochron maps can give a better understanding of hydrocarbon potential.  
687 This section will focus on the hydrocarbon potential of the Muara Sub-basin and Deepwater Tarakan  
688 Basin. The petroleum system elements in the Muara Sub-basin and Deepwater Tarakan Basin are  
689 described in this section. Schematic cartoons showing play cross-sections across the depocentre of the  
690 Muara Sub-basin and Deepwater Tarakan Basin are summarized in Figure 24 and Figure 25.

691

### 692 **5.1 Source rock**

693 In the Muara Sub-basin, oil and gas shows have been encountered by several exploration wells through  
694 the carbonate build ups (e.g. Taballar-1, Karang Besar-1, and Segitiga-1) as reported by several authors  
695 (Achmad and Samuel, 1984; Lentini and Darman, 1996; PERTAMINA-BPPKA, 1996), implying the



696 presence of source rocks charging the reservoir. Possible potential source rocks in this basin are the  
697 Eocene Maliau Mudstone (PERTAMINA-BPPKA, 1996; Wilson et al., 2007) which consists of predominantly  
698 dark-grey shales of an upper bathyal environment (Wilson et al., 2007). Another potential source is the  
699 planktonic shales and marls of the deep marine Oligocene Mangkabua Formation and Miocene Birang  
700 Formation (PERTAMINA-BPPKA, 1996).

701

702 Possible source rocks in the Tarakan Basin include coals and siltstones of the Middle Miocene Meliat and  
703 Late Miocene Formations (PERTAMINA-BPPKA, 1996; Wight et al., 1992). The Tarakan Basin has more  
704 than 14 discoveries of oil and gas fields (PERTAMINA-BPPKA, 1996) generated from source rocks of  
705 lacustrine, coastal plain, and deltaic deposits (PERTAMINA-BPPKA, 1996). There are very limited  
706 information and exploration in the Deepwater Tarakan Basin. Possible source rocks in the Deepwater  
707 Tarakan Basin include deep marine shales of Eocene to Miocene age. According to BP (2000) internal  
708 report of the Bougainville-1 well summary in the Deepwater Tarakan Basin, there was poor hydrocarbon  
709 shows with minor gas peaks only. The section below detachment possibly mature source rock but no  
710 migration path to charge to the anticline (BP, 2000). Thus, the Bougainville-1 well is considered as dry  
711 well and it is interpreted that the well was drilled far down dip of the crest of the anticline structure and  
712 below the hydrocarbon water contacts (Atzeni and Guritno, 2003).

713

714 However, the Aster-1 well in the Deepwater Tarakan Basin shows promising result. According to Atzeni  
715 and Guritno (2003), the Aster-1 well, which was situated relatively near the crestal position of the  
716 anticline structure, consists of 6 oil and gas levels with the main discovery level was the Upper Miocene  
717 AST200 that has 10m of oil. The biomarkers of the oil sample show a terrestrial origin of the source rock  
718 generated the oil (Atzeni and Guritno, 2003). The oil and gas discovery from Aster-1 well indicates the  
719 effectiveness of the petroleum system in the Deepwater Tarakan Basin (Atzeni and Guritno, 2003).

720

## 721 **5.2 Reservoir**

722 Oligo-Miocene carbonate in the Muara Sub-basin has been targeted as a potential reservoir (Achmad and  
723 Samuel, 1984; Lentini and Darman, 1996; PERTAMINA-BPPKA, 1996; Wilson et al., 1999; Wilson and  
724 Evans, 2002; Wilson et al., 2007). Oil and gas shows have been encountered from this carbonate reservoir

725 as shown in several exploration wells (Taballar-1, Karang Besar-1, and Segitiga-1) reported by previous  
726 authors (Achmad and Samuel, 1984; Lentini and Darman, 1996; PERTAMINA-BPPKA, 1996).

727

728 Average porosity from the wells drilled in the Muara Sub-basin range from 12% in Taballar-1 well up to  
729 about 22% in Karang Besar-1 well (PERTAMINA-BPPKA, 1996). Another potential reservoir in the Muara  
730 Sub-basin is deep marine sandstones of Late Oligocene and Miocene age. Other possibilities are Miocene  
731 shallow marine sandstones in the landward area. However, in the Muara Sub-basin, the shallow water  
732 area was mostly covered by carbonate during the Oligo-Miocene (PERTAMINA-BPPKA, 1996).

733

734 In the Tarakan Basin, oil and gas has mainly been produced from Miocene sandstones of the Tabul  
735 Formation (Achmad and Samuel, 1984; Lentini and Darman, 1996; PERTAMINA-BPPKA, 1996) which  
736 were primary objectives for the establishment of production at the Sembakung Field (25 MMBO) in 1976  
737 by Arco (Lentini and Darman, 1996). However, little exploration has occurred in the Deepwater Tarakan  
738 Basin.

739

740 Potential reservoirs in the Deepwater Tarakan Basin include Oligo-Miocene deep marine sandstones.  
741 Quartz turbidite sandstones with almost 90% quartz encountered in the Celebes Sea was transported  
742 from the Borneo to the deep marine areas in the east during the Middle-Late Miocene (Nichols and Hall,  
743 1999). Quartz-rich sandstones are usually mature sandstones with good reservoir quality. Direct  
744 Hydrocarbon Indicators (DHI) in the Deepwater Tarakan Basin suggest several potential gas-bearing  
745 formations containing biogenic shallow gas (Figure 22). Furthermore, several DHI resemble Bottom  
746 Stimulating Reflectors (BSR) generated from methane hydrates.

747

748 The reservoir summary from Bougainville-1 well indicates 280m thick Miocene sandstone with individual  
749 thickness of 0.3-23m (with average ~2.5m thick; BP, 2000). It has medium grey sandstones, fine grained,  
750 well sorted, sub-angular to rounded grain, loose-friable, 20-30% porosity, which has deposited in the  
751 overbank to channel levee complex (BP, 2000). Similarly, Atzeni and Guritno (2003) reported the  
752 Miocene sandstone drilled from the Aster-1 well has dark-grey sandstone, very fine to medium grained,  
753 sub-rounded, poorly sorted, poor visible porosity, occasionally good to excellent infer porosity, and  
754 friable. The Aster-1 well penetrated a total of 80m of sandstone with 30m of hydrocarbon pay (13m oil an

755 17m gas; Atzeni and Guritno, 2003). It is interpreted that the depositional environment of Miocene  
756 sandstone in the Aster-1 well was drilled in the submarine mid-lower slope setting, whilst the in the  
757 Bougainville-1 well penetrated a more distal environment of basinal area (Atzeni and Guritno, 2003).

758

### 759 **5.3 Potential trap and seal**

760 In the Muara Sub-basin, the potential traps are mainly stratigraphic traps. Pinch out stratigraphic  
761 trapping geometries mainly occur in Oligo-Miocene marine sandstones isolated by the marine shales as a  
762 seal. Potential depositional relief traps also occur in the Oligocene carbonates sealed by shale and locally  
763 by tight Miocene carbonates.

764

765 Observation in the Deepwater Tarakan Basin indicate several potential stratigraphic and structural traps.  
766 Anticline structures could provide 4-way dip closure with localized pinch outs of Oligo-Miocene deep  
767 marine sandstones are likely trapping systems. In the basinward area, the net to gross of sand to shale is  
768 likely to decrease. Thus, sealing effectiveness could be an issue.

769

### 770 **5.4 Risk and uncertainty**

771 The primary risk in the Muara Sub-basin is the sealing capacity. Poorly lateral continuity of shales leads to  
772 increased uncertainty. Fault sealing may also be a problem. Evidence from several seismic sections  
773 showing Direct Hydrocarbon Indicators (DHI) indicates gas leakages utilizing normal faults to the  
774 younger unit above. Gas escape is interpreted from the Oligocene carbonate unit (Figure 23). This  
775 indication could increase the uncertainty of hydrocarbon accumulation.

776

777 In the Deepwater Tarakan Basin, the primary risk is the hydrocarbon charging (source rock maturation,  
778 generation, and migration timing of the hydrocarbon). For example, if the generation post-dates the toe-  
779 thrust faults, there would be a good trapping system for hydrocarbons. On the other hand, if the timing of  
780 hydrocarbon generation pre-dates the thrust faults, the trapping system would be broken and allow  
781 leaking of hydrocarbons. Again, this will increase the uncertainty of hydrocarbon accumulation.

782

783 **CONCLUSIONS**

784 • There are eight main reflector packages identified in the Muara Sub-basin, i.e.: Unit X (Middle Eocene  
785 and older basement complex); Unit A (Upper Eocene marine siliciclastic); Unit B (Lower Oligocene  
786 carbonates); Unit C (Upper Oligocene marine mudstones); Unit D, Unit E, Unit F, and Unit G are Lower  
787 Miocene-Recent marine sediments.

788

789 • Six main reflector packages are identified in the Deepwater Tarakan Basin, i.e.: Unit X1 (Eocene  
790 basaltic basement equivalent); Unit C1, Unit D1, Unit E1, Unit F1, and Unit G1 are Eocene-Recent  
791 equivalents which consist of deep marine siliciclastic sediments.

792

793 • Two main reflector packages are identified in the North Sulawesi Fold-Thrust Belt, as Upper Unit and  
794 Lower Unit that possibly equivalent with Pleistocene and older formation respectively.

795

796 • There is no continuation of Palu-Koro strike-slip Fault to the Muara Sub-basin and the adjacent area  
797 which was interpreted by previous authors as formed by a transpressional fault system. The NW-SE  
798 structural trend in the Muara Sub-basin (i.e. Maratua Ridge) is an Eocene transform fault active  
799 during spreading of the Celebes Sea which became inactive from the Early Oligocene.

800

801 • Termination of spreading in the Celebes Sea was associated with cessation of rifting in the Muara  
802 Sub-basin and the western part of the Deepwater Tarakan Basin during Middle-Late Eocene. There  
803 was significant sediment supply to both basins between the Early Oligocene to Early Miocene from  
804 central Borneo in the west with significant thermal subsidence in the Muara Sub-basin.

805

806 • Inversion and uplift since Middle Miocene in Borneo led to development of rapidly prograding deltaic  
807 environments in the Muara Sub-basin and Deepwater Tarakan Basin. During the latest Miocene or  
808 Pliocene, loading of the upper part of the prograding delta to the east of the Tarakan Basin caused  
809 development of gravity tectonics in the Deepwater Tarakan Basin.

810

811 • The North Sulawesi Fold-Thrust Belt developed since the latest Miocene or Pliocene associated with  
812 subduction of Celebes Sea beneath North Arm of Sulawesi. The downflexing of Celebes Sea as a result

813 of the subduction and loading of North Sulawesi FTB wedges might allowed gravity tectonics in the  
814 Deepwater Tarakan Basin.

815

816 • During the Pliocene, the Deepwater Tarakan Basin and Muara Sub-basin were dominated by  
817 sedimentation in the prograding delta and the basin as inversion and uplift continued. Gravity  
818 tectonics in the Deepwater Tarakan Basin were not active since Pleistocene.

819

820 • Potential hydrocarbon plays identified within the Muara Sub-basin include an Oligocene carbonate  
821 play and an Oligocene-Miocene shallow to deep marine sandstones play. In the Deepwater Tarakan  
822 Basin, the main potential is an Oligocene-Miocene deep marine sandstone play. Sealing effectiveness  
823 and timing of hydrocarbon generation are the main risks in both areas which lead to high uncertainty.

824

## 825 **ACKNOWLEDGEMENTS**

826 The first author would like to thank the SE Asia Research Group (SEARG) for the scholarship opportunity  
827 during the MSc and for continued support during the final project. SEARG is funded by consortium of oil  
828 companies. We are grateful to PGS for the generous provision of 2D seismic data and GeoData Ventures  
829 Pte Ltd for the multibeam bathymetry data under an academic license agreement. We would also like to  
830 thank The KINGDOM Software 8.8 as the main software that used in this project.

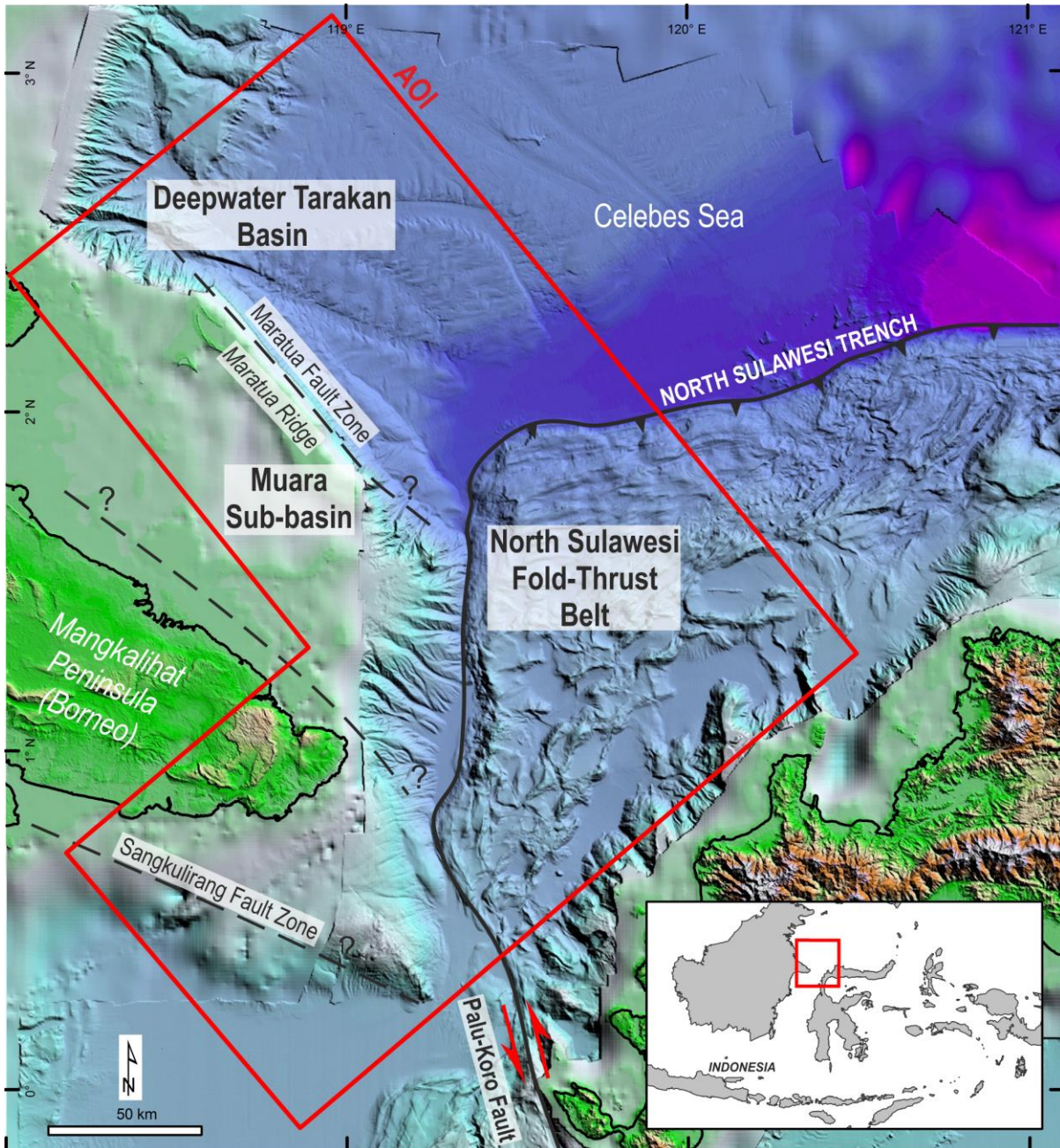
831

## 832 **REFERENCES**

- 833 ACHMAD, Z. & SAMUEL, L. Stratigraphy and depositional cycles in the NE Kalimantan Basin. 13th Annual  
834 Convention 1984 Jakarta. Proceedings, Indonesian Petroleum Association, 12 pp.
- 835 ADVOKAAT, E. L. 2015. *Neogene extension and exhumation in NW Sulawesi*. Unpublished Ph.D. Thesis,  
836 Royal Holloway University of London.
- 837 ADVOKAAT, E. L., HALL, R., WHITE, L. T., WATKINSON, I. M., RUDYAWAN, A. & BOUDAGHER-FADEL, M. K.  
838 2017. Miocene to recent extension in NW Sulawesi, Indonesia. *Journal of Asian Earth Science*.
- 839 ATZENI, G. L. & GURITNO, E. 2003. Aster-1 Final Geological Report. ENI Bukat.
- 840 BELLIER, O., SEBRIER, M., SEWARD, D., BEAUDOUIN, T., VILLENEUVE, M. & PUTRANTO, E. 2006. Fission  
841 track and fault kinematics analyses for new insight into the Late Cenozoic tectonic regime  
842 changes in West-Central Sulawesi (Indonesia). *Tectonophysics*, 413, 201-220.
- 843 BP 2000. Bougainville-1 Ambalat PSC, Deepwater Tarakan Basin - Makassar Strait, Indonesia. Shell-BP-  
844 Lasmo-Unocal.
- 845 CAMP, W. K., GURITNO, E. E., DRAJAT, D. & WILSON, M. E. Middle-lower Eocene turbidites: a new  
846 deepwater play concept, Kutei Basin, East Kalimantan, Indonesia. 33rd Annual Convention 2009  
847 Jakarta. Proceedings, Indonesian Petroleum Association, 14 pp.
- 848 CHAMBERS, J. & DALEY, T. E. 1997. A tectonic model for the onshore Kutai Basin, East Kalimantan. *In:*  
849 *Fraser, A. J., Matthews, S. J., Murphy, R. W., (Eds), Petroleum Geology of Southeast Asia*, 126.
- 850 CHUNG-HWA, P., TAMAKI, K. & KOBAYASHI, K. 1990. Age-depth correlation of the Philippine Sea back-arc  
851 basins and other marginal basins in the world. *Tectonophysics*, 181, 351-371.

- 852 CLOKE, I., MILSOM, J. & BLUNDELL, D. 1999a. Implications of gravity data from East Kalimantan and the  
853 Makassar Straits: a solution to the origin of the Makassar Straits? *Journal of Asian Earth Sciences*,  
854 17, 61-78.
- 855 CLOKE, I., MOSS, S. & CRAIG, J. 1999b. Structural controls on the evolution of the Kutai Basin, East  
856 Kalimantan. *Journal of Asian Earth Sciences*, 17, 137-156.
- 857 DALY, M. C., COOPER, M. A., HOOPER, B. G. D., WILSON, I. & SMITH, D. G. 1999. Cenozoic plate tectonics  
858 and basin evolution in Indonesia. *Marine and Petroleum Geology*, 8.
- 859 DJAJADIHARDJA, Y. S., TAIRA, A., TOKUYAMA, H., AOIKE, K., REICHERT, C., BLOCK, M., SCHLUTER, H. U. &  
860 NEBEN, S. 2004. Evolution of an accretionary complex along the north arm of the island of  
861 Sulawesi, Indonesia. *Island Arc*, 13, 1-17.
- 862 FRASER, T. H., JACKSON, B. A., BARBER, P. M., BAILLIE, P. & MYERS, K. The West Sulawesi Fold Belt and  
863 Other New Plays Within the North Makassar Straits—A Prospectivity Review. 29th Annual  
864 Convention 2003 Jakarta. Proceedings, Indonesian Petroleum Association, 19 pp.
- 865 GAFEIRA, J. 2010. A geomorphological interpretation of multibeam data from the nearshore area between  
866 Belfast Lough and Cushendun, Northern Ireland. *Marine Geoscience Programme Commissioned*  
867 *Report CR/10/075*. British Geological Survey Commissioned Report.
- 868 GOVERS, R. & WORTEL, M. J. 2005. Lithosphere tearing at STEP faults: response to edges of subduction  
869 zones. *Earth and Planetary Science Letters*, 236, 505-523.
- 870 HALL, R. 1996. Reconstructing Cenozoic SE Asia. *Geological Society, London, Special Publications*, 106,  
871 153-184.
- 872 HALL, R. 2002. Cenozoic geological and plate tectonic evolution of SE Asia and the SW Pacific: computer-  
873 based reconstructions, model and animations. *Journal of Asian Earth Sciences*, 20, 353-431.
- 874 HALL, R. 2011. Australia–SE Asia collision: plate tectonics and crustal flow. *Geological Society, London,*  
875 *Special Publications*, 355, 75-109.
- 876 HALL, R. 2012. Late Jurassic–Cenozoic reconstructions of the Indonesian region and the Indian Ocean.  
877 *Tectonophysics*, 570, 1-41.
- 878 HALL, R., CLOKE, I. R., NUR'AINI, S., PUSPITA, S. D., CALVERT, S. J. & ELDERS, C. F. 2009. The North  
879 Makassar Straits: what lies beneath? *Petroleum Geoscience*, 15, 147-158.
- 880 HAMILTON, W. B. 1979. *Tectonics of the Indonesian region*, US Govt. Print. Off.
- 881 HAQ, B. U., HARDENBOL, J. & VAIL, P. R. 1988. Mesozoic and Cenozoic chronostratigraphy and cycles of  
882 sea-level change.
- 883 HIDAYATI, S., GURITNO, E., ARGENTON, A., ZIZA, W. & CAMPANA, I. D. 2007. Re-visited structural  
884 framework of the Tarakan sub-basin Northeast Kalimantan - Indonesia. *Indonesian Petroleum*  
885 *Association, Proceedings 31st Annual Convention*, 255-272.
- 886 ICS. 2017. *International Chronostratigraphic Chart* [Online]. International Commission on Stratigraphy.  
887 Available: <http://www.stratigraphy.org/index.php/ics-chart-timescale> [Accessed May 15th  
888 2017].
- 889 LENTINI, M. R. & DARMAN, H. Aspects of the Neogene tectonic history and hydrocarbon geology of the  
890 Tarakan Basin. 27th Annual Convention, 1996 Jakarta. Proceedings, Indonesian Petroleum  
891 Association, 11 pp.
- 892 LETOUZEY, J., WERNER, P. & MARTY, A. 1990. Fault reactivation and structural inversion. Backarc and  
893 intraplate compressive deformations. Example of the eastern Sunda shelf (Indonesia).  
894 *Tectonophysics*, 183, 341-362.
- 895 MITCHUM JR, R., VAIL, P. & THOMPSON III, S. 1977. Seismic stratigraphy and global changes of sea level:  
896 Part 2. The depositional sequence as a basic unit for stratigraphic analysis: Section 2. Application  
897 of seismic reflection configuration to stratigraphic interpretation.
- 898 MORLEY, C. K., KING, R., HILLIS, R., TINGAY, M. & BACKE, G. 2011. Deepwater fold and thrust belt  
899 classification, tectonics, structure and hydrocarbon prospectivity: A review. *Earth-Science*  
900 *Reviews*, 104, 41-91.
- 901 MURAUCHI, S., LUDWIG, W., DEN, N., HOTTA, H., ASANUMA, T., YOSHII, T., KUBOTERA, A. & HAGIWARA,  
902 K. 1973. Structure of the Sulu Sea and the Celebes Sea. *Journal of Geophysical Research*, 78, 3437-  
903 3447.
- 904 NICHOLS, G. & HALL, R. 1999. History of the Celebes Sea Basin based on its stratigraphic and  
905 sedimentological record. *Journal of Asian Earth Sciences*, 17, 47-59.
- 906 NUR'AINI, S., HALL, R. & ELDERS, C. F. Basement Architecture and Sedimentary Fill of the North Makassar  
907 Straits Basin. 30th Annual Convention, 2005 Jakarta. Proceedings, Indonesian Petroleum  
908 Association, 14 pp.

909 ORANGE, D. L., TEAS, P. A. & DECKER, J. SS: Multibeam Backscatter-Insights into Marine Geological  
910 Processes and Hydrocarbon Seepage. Offshore Technology Conference, 2010. Offshore  
911 Technology Conference Houston, Texas, USA, OTC 20860 1-22.  
912 PERTAMINA-BPPKA 1996. *Petroleum geology of Indonesian Basins: principles, methods, and application*,  
913 Jakarta, Pertamina BPPKA (Foreign Contractors Ventures Development Body).  
914 PIETERS, P. E., PIGRAM, C. J., TRAIL, D. S., DOW, D. B., RATMAN, N. & SUKAMTO, R. 1983. The stratigraphy  
915 of western Iran Jaya. *Bulletin of the Geological Research and Development Centre*, 8, 14-48.  
916 PUTRA, P. R., SAPIIE, B. & RAMDHAN, A. M. 2018. PS Relationship Between Pore Pressure and Structural  
917 Model in "Passive Margin" Offshore Tarakan Sub-Basin, Northeast Kalimantan, Indonesia.  
918 RANGIN, C., SILVER, E. A., VON BREYMAN, M. T. & AL., E. 1990. Proceedings of the Ocean Drilling Program.  
919 *Initial Reports*.  
920 RUDYAWAN, A. 2016. *Neogene stratigraphy, structure, and magmatism of the central North Arm of*  
921 *Sulawesi, Indonesia*. Unpublished Ph.D. Thesis, Royal Holloway University of London.  
922 SATYANA, A. H., NUGROHO, D. & SURANTOKO, I. 1999. Tectonic controls on the hydrocarbon habitats of  
923 the Barito, Kutei, and Tarakan Basins, Eastern Kalimantan, Indonesia: major dissimilarities in  
924 adjoining basins. *Journal of Asian Earth Sciences*, 17, 99-122.  
925 SILVER, E. A., MCCAFFREY, R. & SMITH, R. B. 1983. Collision, rotation, and the initiation of subduction in  
926 the evolution of Sulawesi, Indonesia. *Journal of Geophysical Research: Solid Earth*, 88, 9407-9418.  
927 SILVER, E. A. & RANGIN, C. 1. LEG 124 Tectonic synthesis. Proceedings of the Ocean Drilling Program,  
928 Scientific Results, 1991. 3-9.  
929 SOCQUET, A., VIGNY, C., CHAMOT-ROOKE, N., SIMONS, W., RANGIN, C. & AMBROSIUS, B. 2006. India and  
930 Sunda plates motion and deformation along their boundary in Myanmar determined by GPS.  
931 *Journal of Geophysical Research: Solid Earth*, 111.  
932 SUNARYO, R., MARTODJOJO, S. & WAHAB, A. 1988. Detailed geological evaluation of the hydrocarbon  
933 prospects in the Bungalun area, East Kalimantan. *Indonesian Petroleum Association, Proceedings*  
934 *17th annual convention, Jakarta, 1988*, 1, 423-446.  
935 SURMONT, J., LAJ, C., KISSEL, C., RANGIN, C., BELLON, H. & PRIADI, B. 1994. New paleomagnetic  
936 constraints on the Cenozoic tectonic evolution of the North Arm of Sulawesi, Indonesia. *Earth and*  
937 *Planetary Science Letters*, 121, 629-638.  
938 VIGNY, C., PERFETTINI, H., WALPERSDORF, A., LEMOINE, A., SIMONS, W., VAN LOON, D., AMBROSIUS, B.,  
939 STEVENS, C., MCCAFFREY, R. & MORGAN, P. 2002. Migration of seismicity and earthquake  
940 interactions monitored by GPS in SE Asia triple junction: Sulawesi, Indonesia. *Journal of*  
941 *Geophysical Research: Solid Earth*, 107.  
942 WALPERSDORF, A., RANGIN, C. & VIGNY, C. 1998. GPS compared to long-term geologic motion of the  
943 north arm of Sulawesi. *Earth and Planetary Science Letters*, 159, 47-55.  
944 WATKINSON, I. M. 2011. Ductile flow in the metamorphic rocks of central Sulawesi. In: HALL, R., COTTAM,  
945 M. A. & WILSON, M. E. J. (eds.) *The SE Asian Gateway: History and Tectonics of the Australia-Asia*  
946 *collision*.  
947 WATKINSON, I. M. & HALL, R. 2016. Fault systems of the eastern Indonesian triple junction: evaluation of  
948 Quaternary activity and implications for seismic hazards. *Geological Society, London, Special*  
949 *Publications*, 441, SP441. 8.  
950 WEISSEL, J. K. 1980. Evidence for Eocene oceanic crust in the Celebes Basin. *The Tectonic and Geologic*  
951 *Evolution of Southeast Asian Seas and Islands*, 37-47.  
952 WIGHT, A., HARE, L. & REYNOLDS, J. 1992. Tarakan Basin, NE Kalimantan, Indonesia: a century of  
953 exploration and future potential. *Bulletin of the Geological Society of Malaysia*, 33, 265-288.  
954 WILSON, M., CHAMBERS, J., EVANS, M., MOSS, S. & NAS, D. S. 1999. Cenozoic carbonates in Borneo: case  
955 studies from northeast Kalimantan. *Journal of Asian Earth Sciences*, 17, 183-201.  
956 WILSON, M. E. & EVANS, M. J. 2002. Sedimentology and diagenesis of Tertiary carbonates on the  
957 Mangkalihat Peninsula, Borneo: implications for subsurface reservoir quality. *Marine and*  
958 *Petroleum Geology*, 19, 873-900.  
959 WILSON, M. E., EVANS, M. J., OXTOBY, N. H., NAS, D. S., DONNELLY, T. & THIRLWALL, M. 2007. Reservoir  
960 quality, textural evolution, and origin of fault-associated dolomites. *AAPG bulletin*, 91, 1247-1272.  
961



962

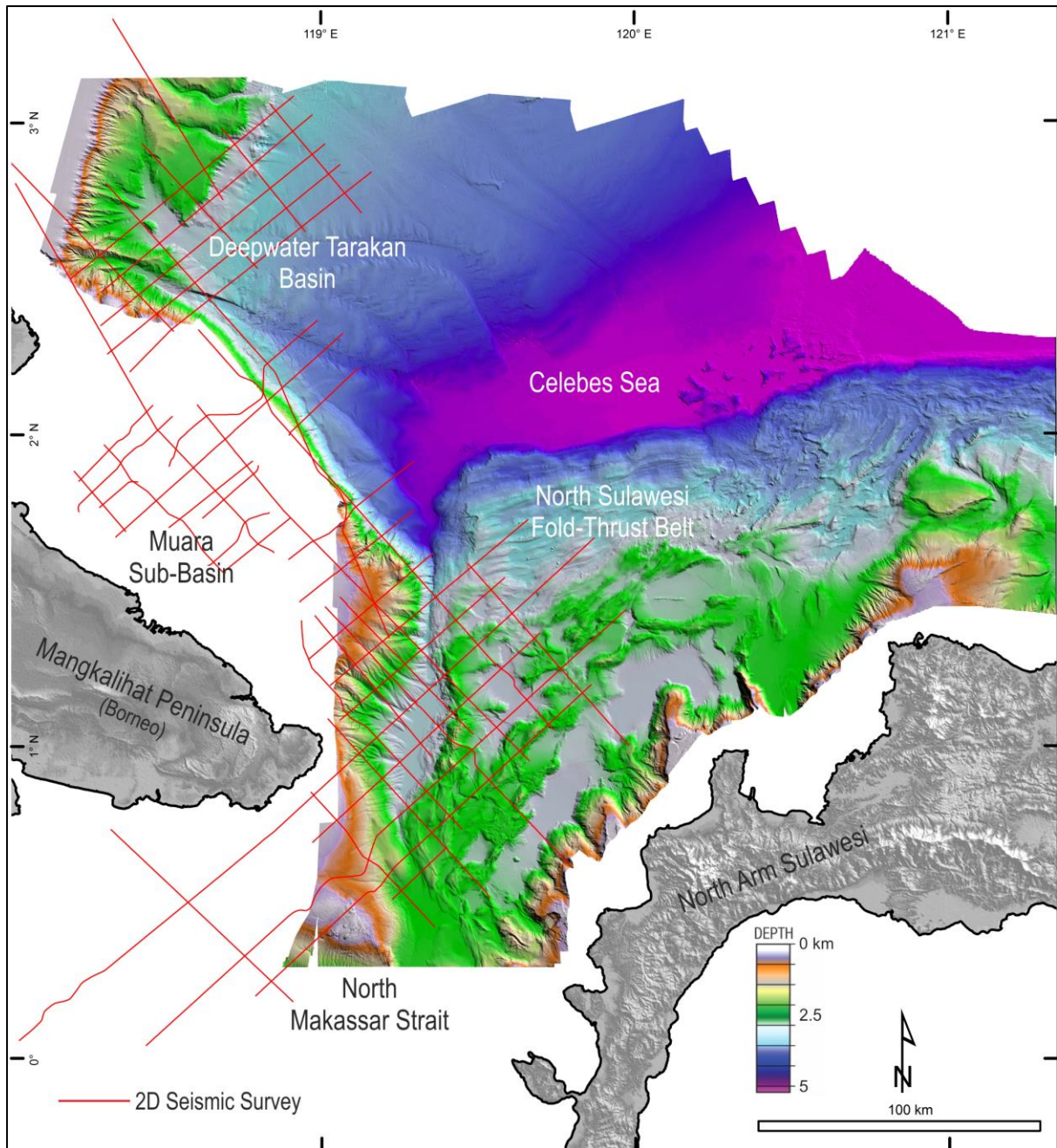
963

964

965

Figure 1. ASTER DEM, bathymetry, and gravity image of study area showing topography, regions, basin or sub-basin, and major tectonic province (Advokaat, 2015; Camp et al., 2009; Cloke et al., 1999b). Red box highlighting the area of interest (AOI).

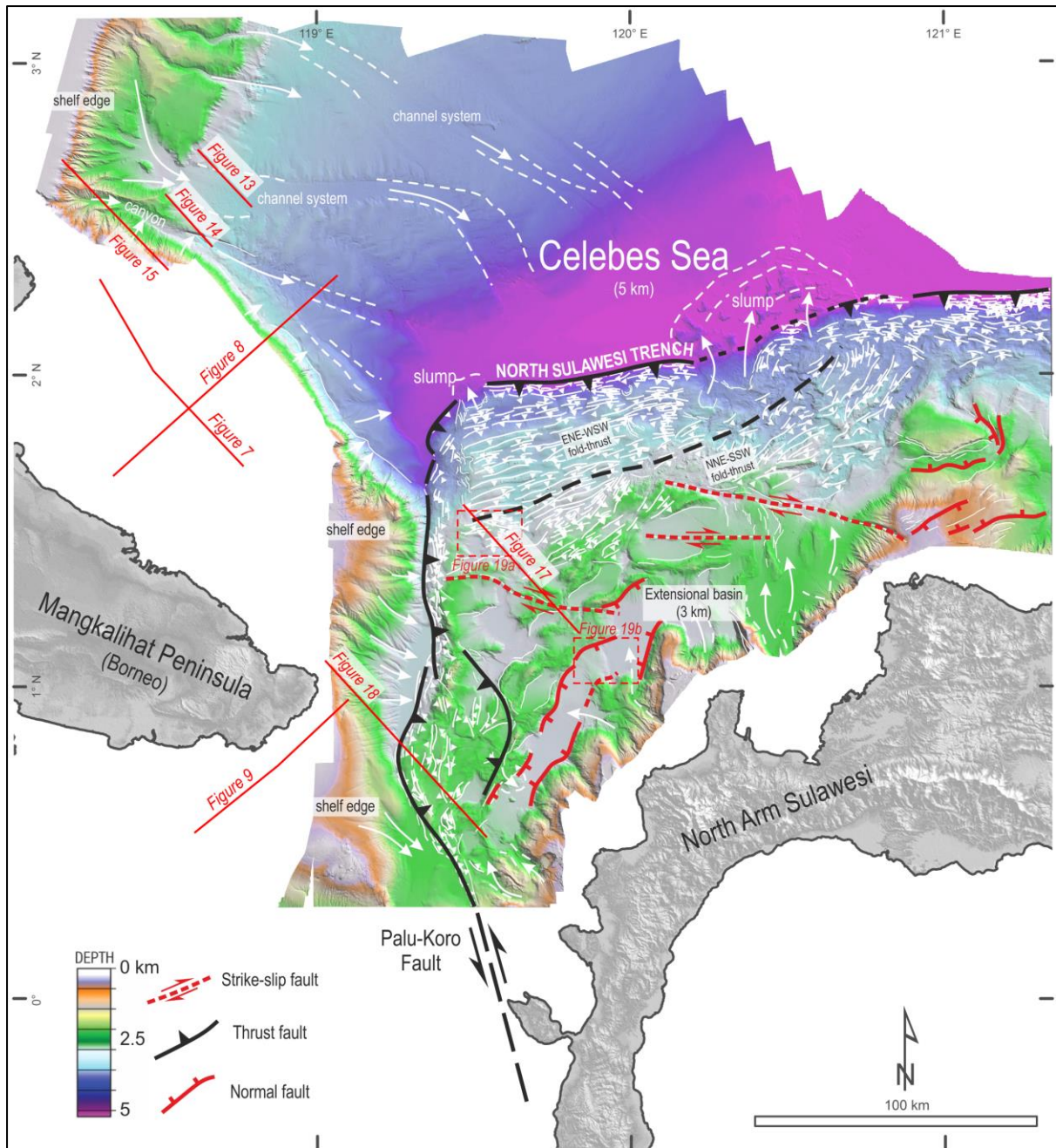




966

967 Figure 2. DEM on land from SRTM (Shuttle Radar Topographic Mission) with the multibeam bathymetry

968 map and 2D seismic survey lines used in this study.



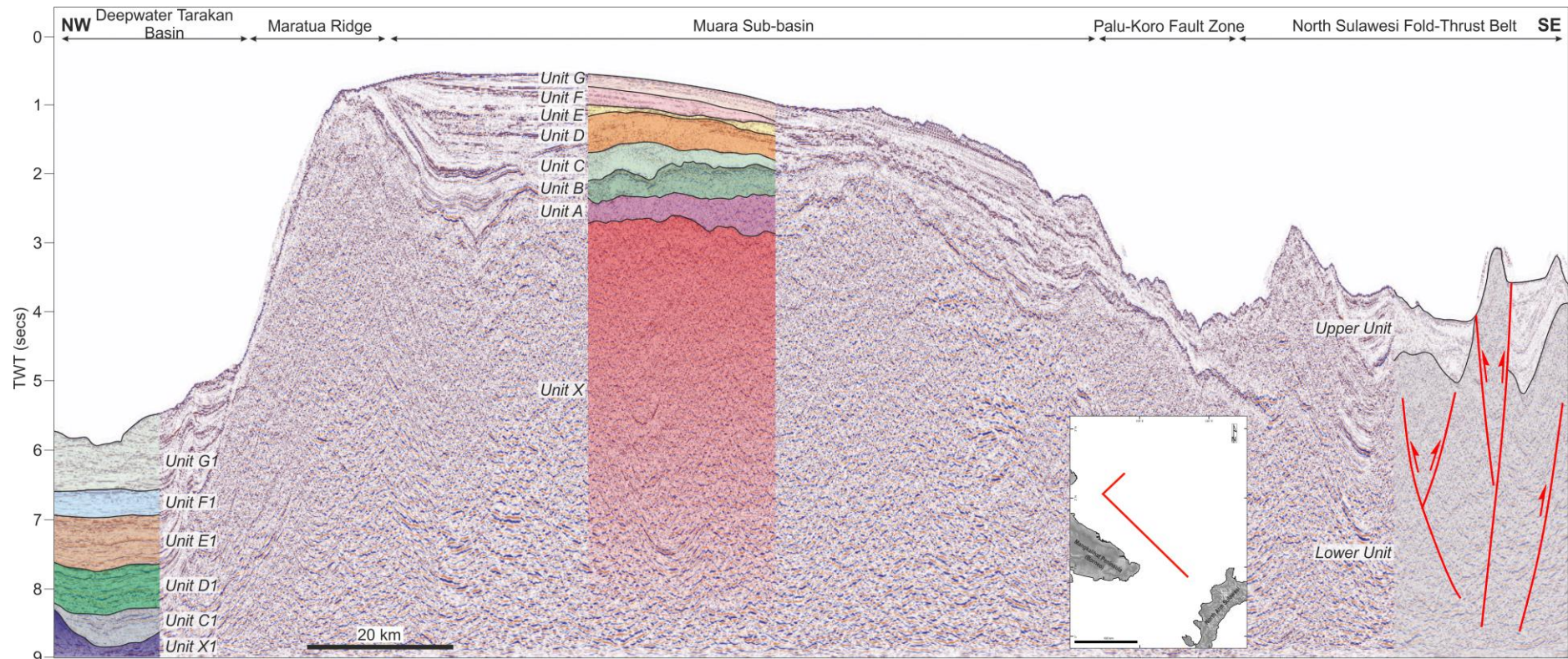
969

970 Figure 3. Combined DEM from SRTM map with a shaded-relief map of interpreted multibeam bathymetry

971 with exceptional details of sedimentary and structural features described in this chapter. Red lines

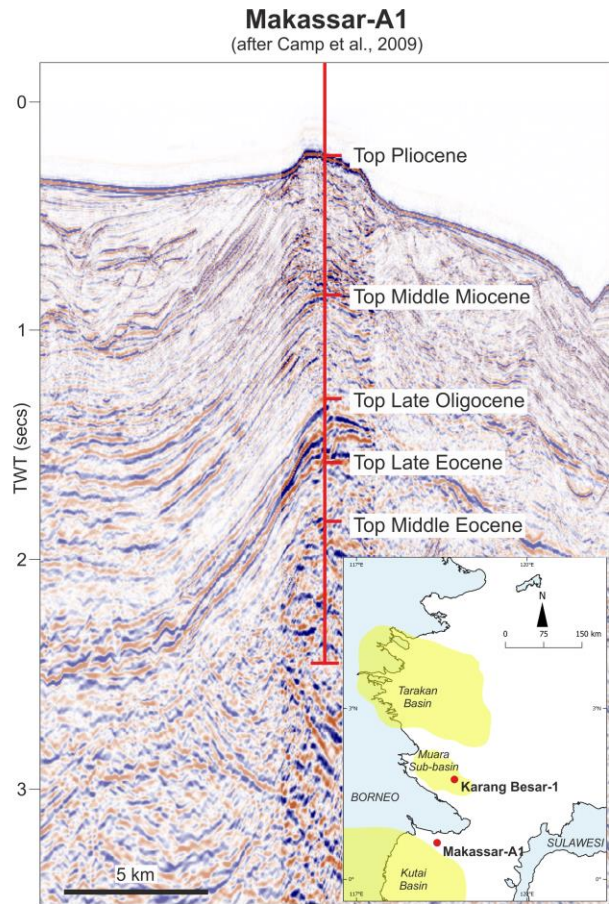
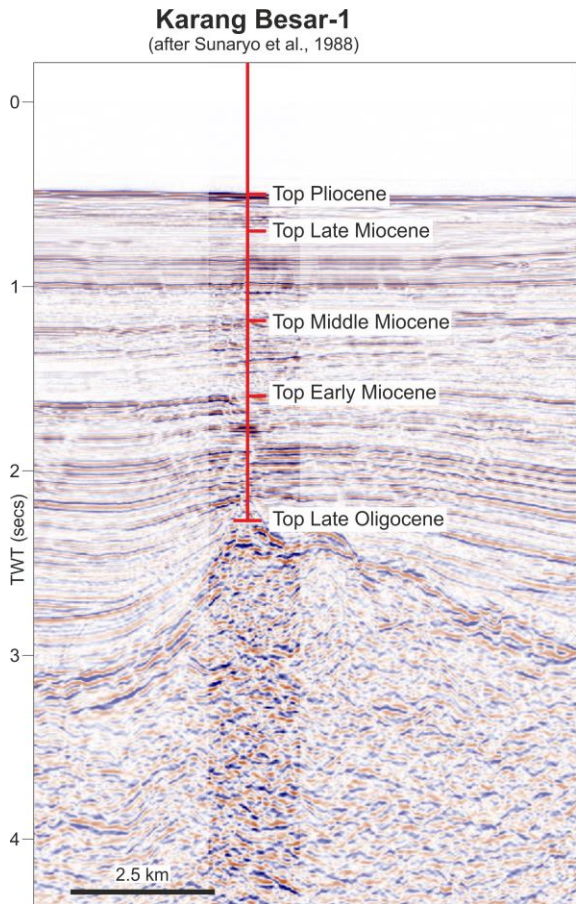
972 indicate seismic section presented in this paper. Illumination direction from NE.

973



974

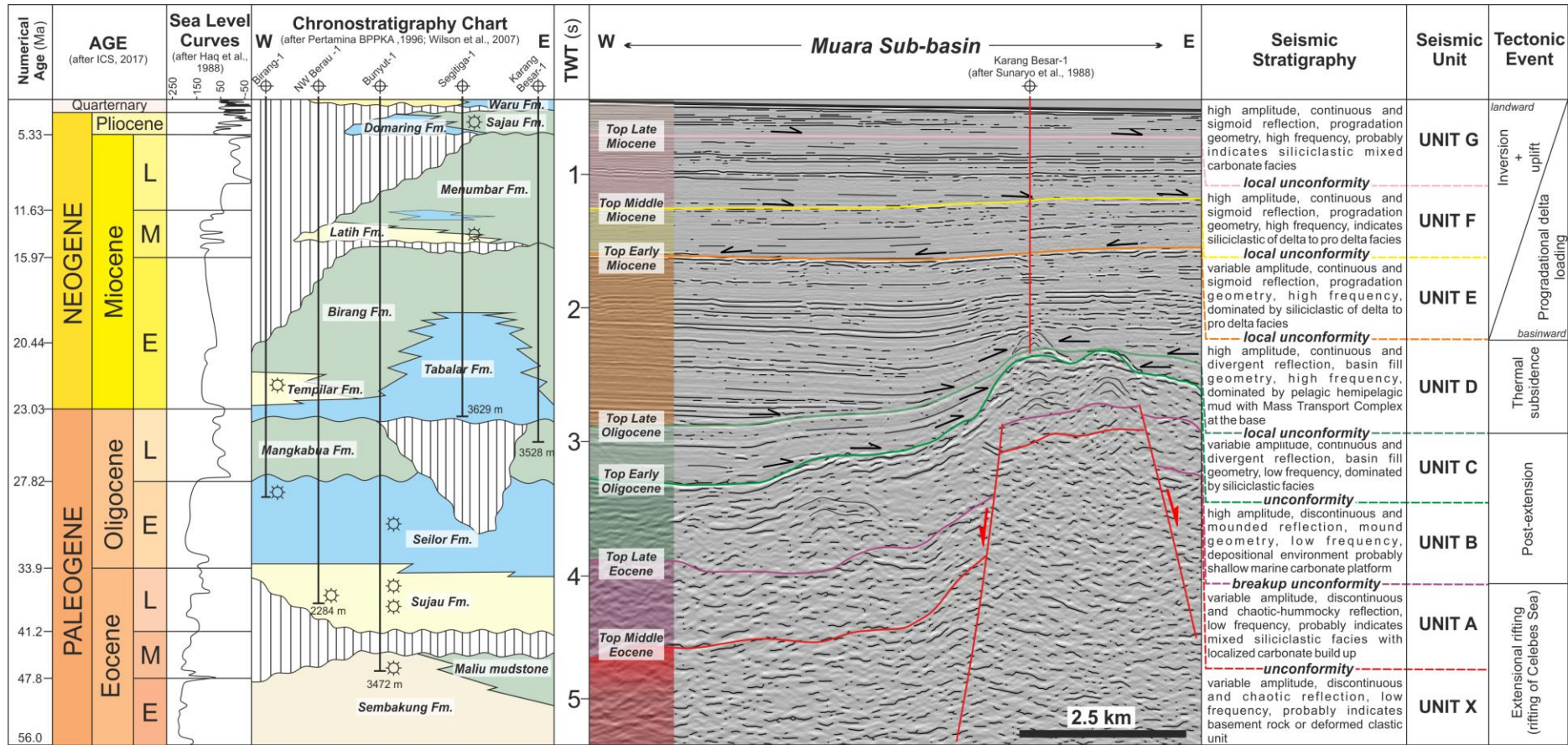
975 Figure 4. Composite seismic line across Deepwater Tarakan Basin, Muara Sub-basin, and North Sulawesi Fold-Thrust Belt showing different seismic stratigraphic  
976 units for each area.



977

978 Figure 5. Stratigraphic well control used in this paper for the Muara Sub-basin (modified after Camp et al.,

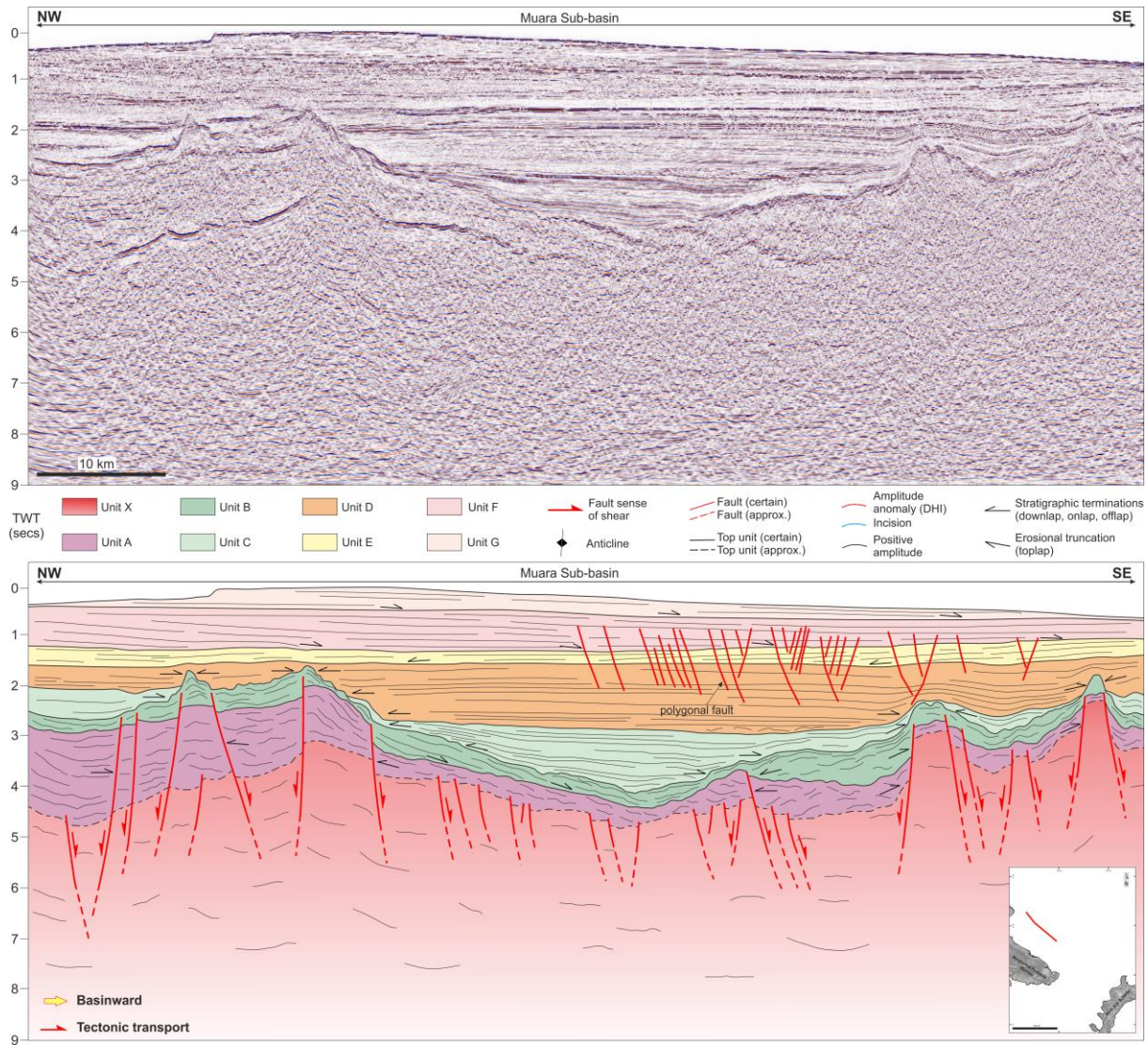
979 2009; Sunaryo et al., 1988).



980

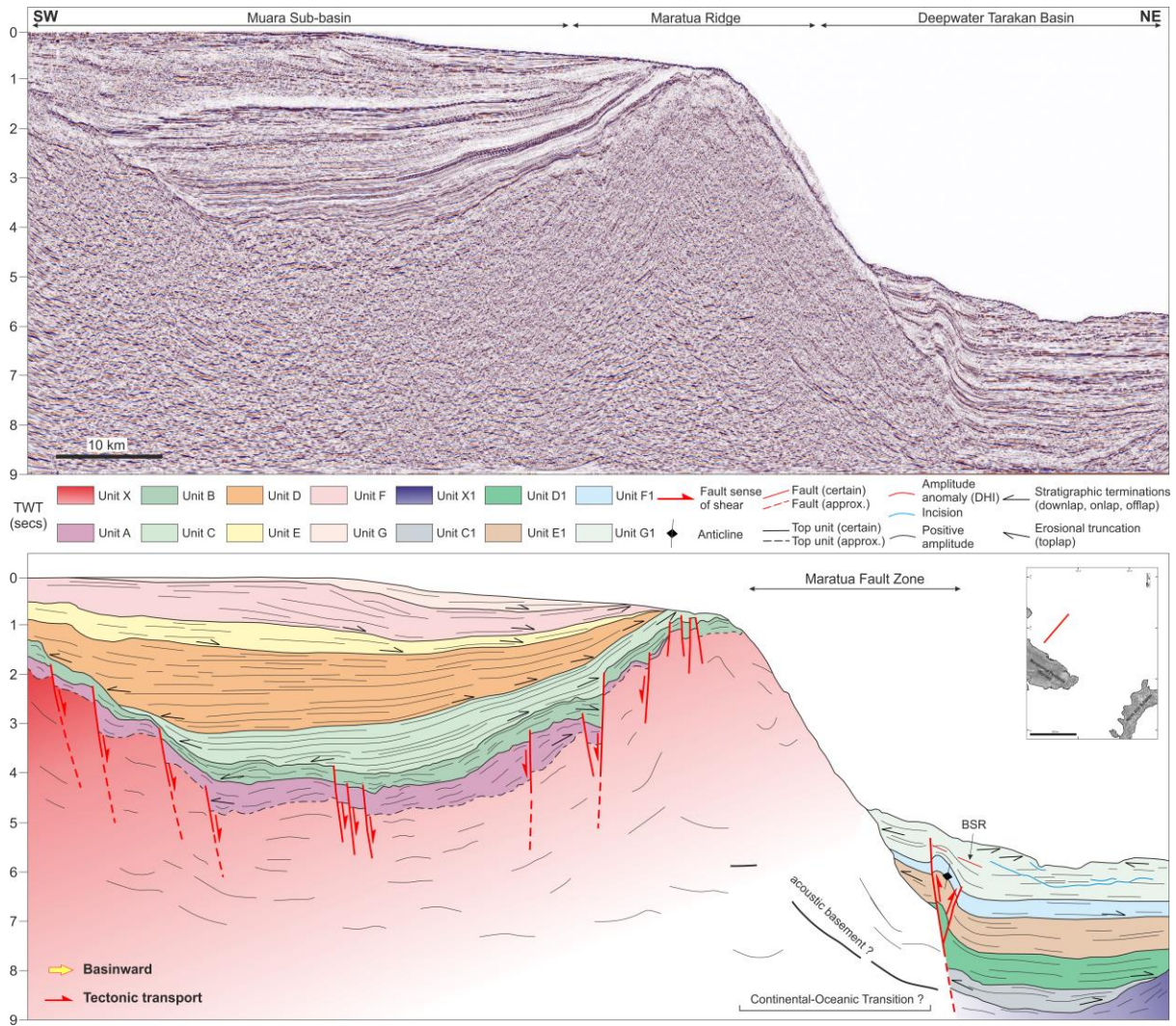
981 Figure 6. Summarized seismic stratigraphy units of the Muara Sub-basin modified from various sources (Haq et al., 1988; ICS, 2017; PERTAMINA-BPPKA, 1996;

982 Wilson et al., 2007; Sunaryo et al., 1988).



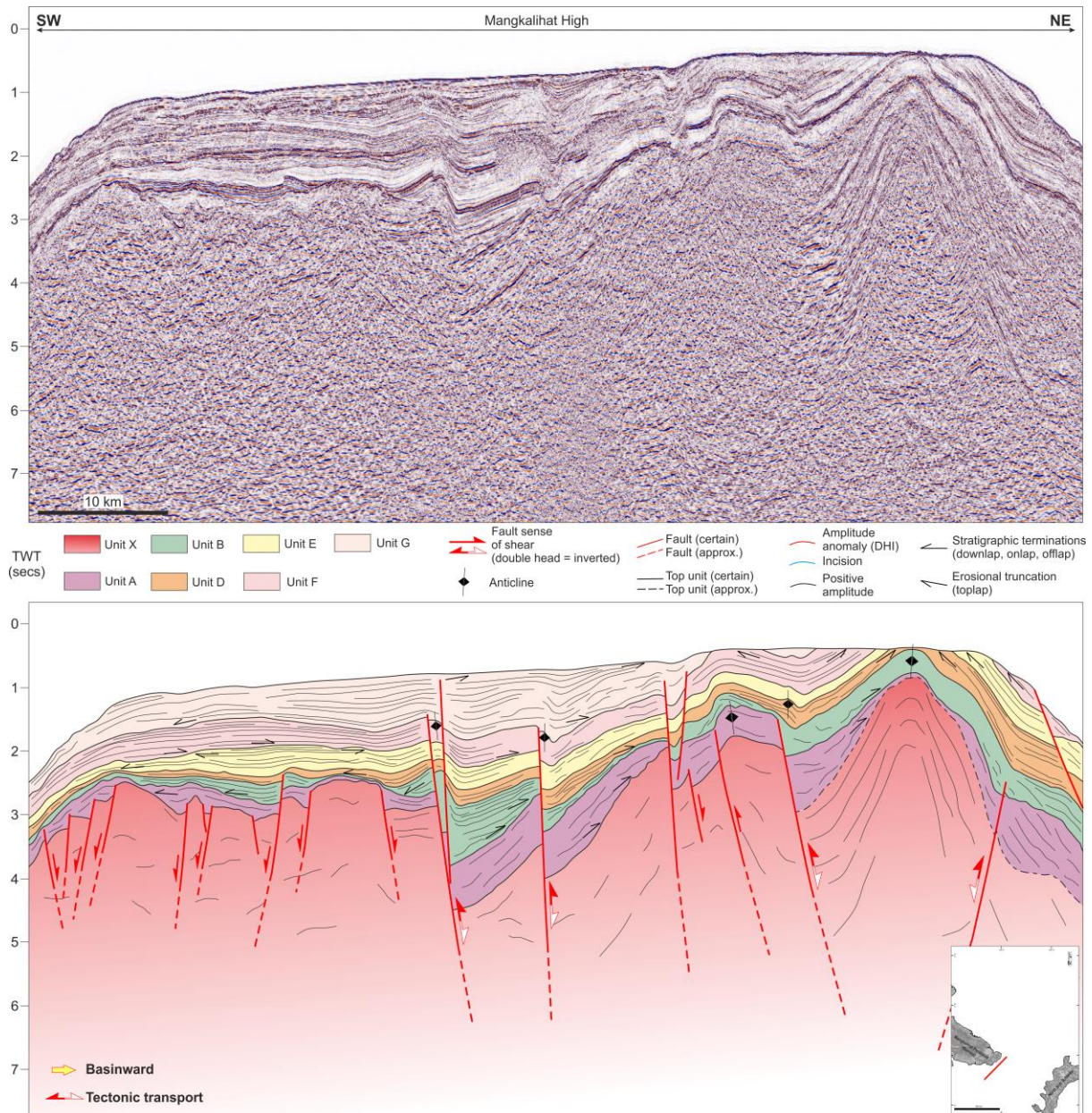
983

984 Figure 7. Uninterpreted (above) and interpreted (below) NW-SE seismic section following approximately  
 985 the axis of Muara Sub-basin. The basin geometry is strongly controlled by the underlying basement  
 986 configuration (Unit X). Carbonate build-up features in Unit B were seated on top of structural high and  
 987 buried by young sedimentary strata.



988

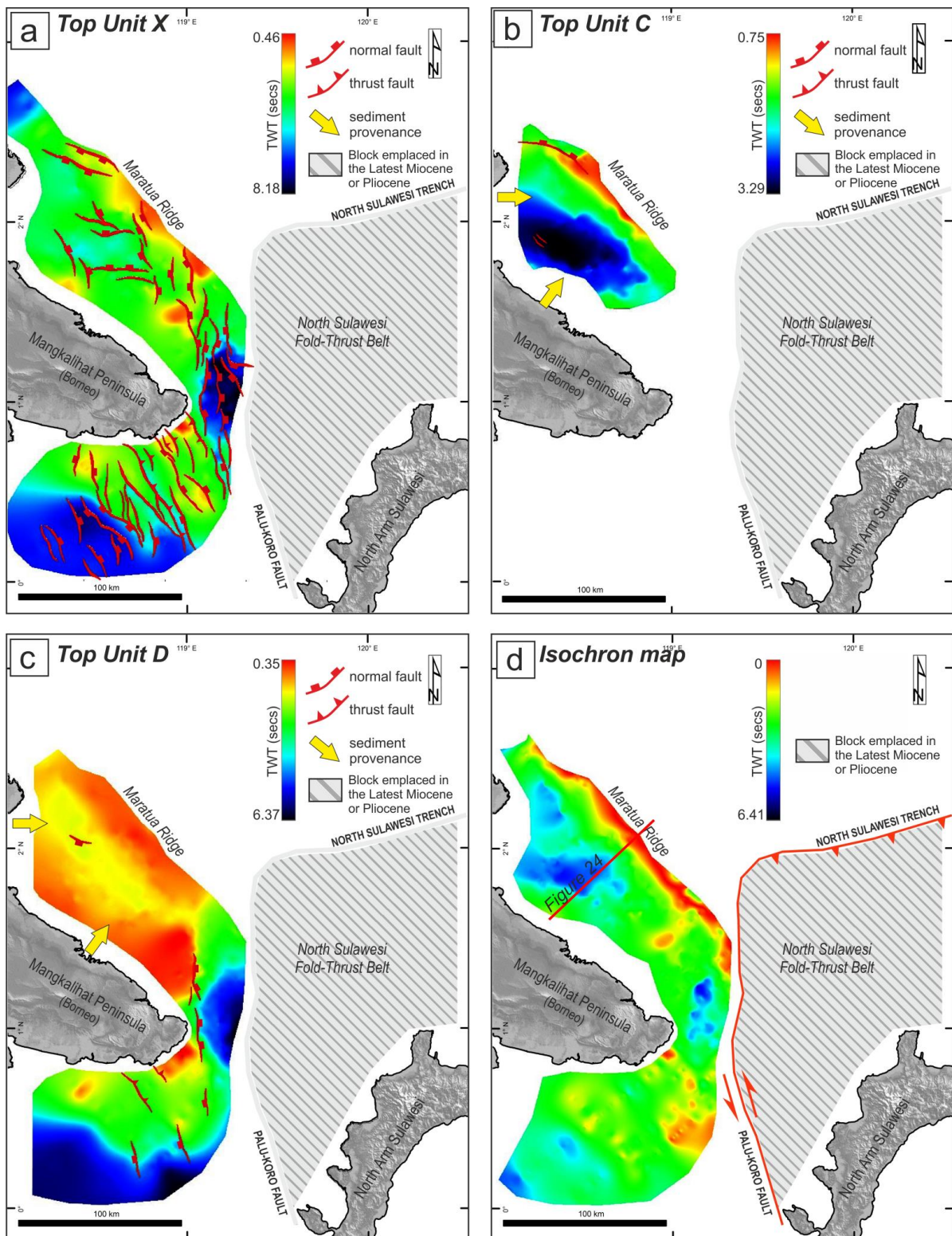
989 Figure 8. Uninterpreted (above) and interpreted (below) NE-SW seismic section through Muara Sub-  
 990 basin, Maratua Ridge, and Deepwater Tarakan Basin. The great amount of sediment thicknesses in the  
 991 Muara Sub-basin were deposited since Early Miocene following subsidence and rapid sedimentation in  
 992 such narrow basin. The sediment in the Deepwater Tarakan Basin is separated to the Muara Sub-basin by  
 993 Maratua Ridge as prominent structural high.



994

995 Figure 9. Uninterpreted (above) and interpreted (below) NE-SW seismic section from the eastern end of  
 996 Mangkalihah High. Inverted extensional fault were observed from the seismic section where the inversion  
 997 event is interpreted to have occur since Middle Miocene as shown by erosional truncation at Top Unit E  
 998 (Top Middle Miocene) as a result of Mangkalihah uplift. These also contributes to the prograding shelf in  
 999 the Muara Sub-basin as observed at seismic stratigraphy Unit E, F, and G shown in Figure 8.





1000

1001 Figure 10. Subsurface map in the Muara Sub-basin and adjacent area. (a) Depth to Top Unit X structure

1002 map highlights basal unconformity in the Muara Sub-basin were controlled by broadly NNW-SSE

1003 structural trend. Minor thrust faults were observed in the eastern most of Mangkalihat Peninsula as

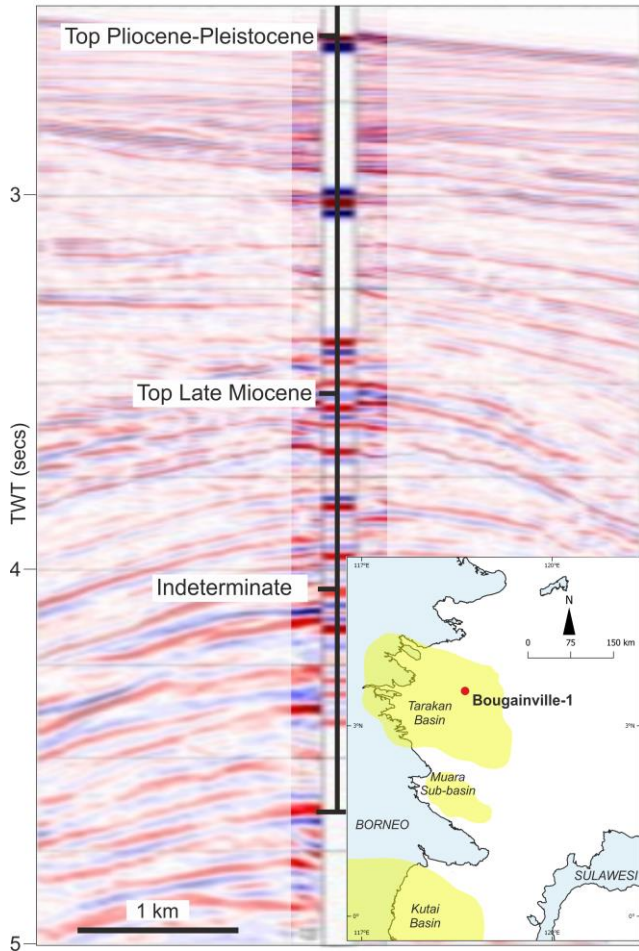
1004 inverted normal fault which also seen from the seismic profile. (b) Local infilled of Unit C in the Muara

1005 Sub-basin following the post-extension in the area. (c) Widespread deposition of Unit D during Early

1006 Miocene with not much deformation in the Muara Sub-basin. (d) Total sediment thickness map showing  
1007 the NW-SE trend of the axial Muara Sub-basin.  
1008

# Bougainville-1

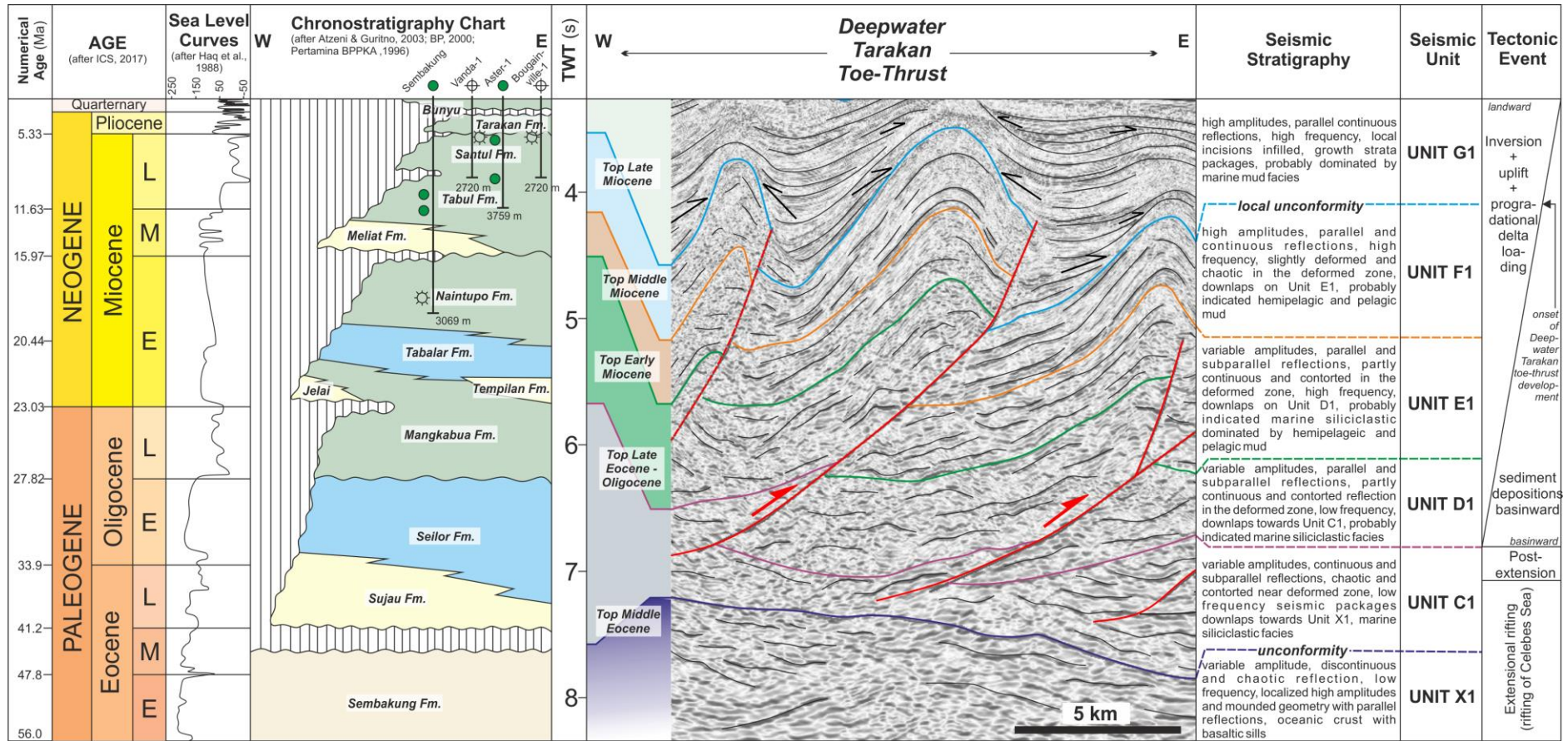
(after BP, 2000; unpublished manuscript)



1009

1010 Figure 11. Stratigraphic well control used in this paper for the Deepwater Tarakan Basin (modified after

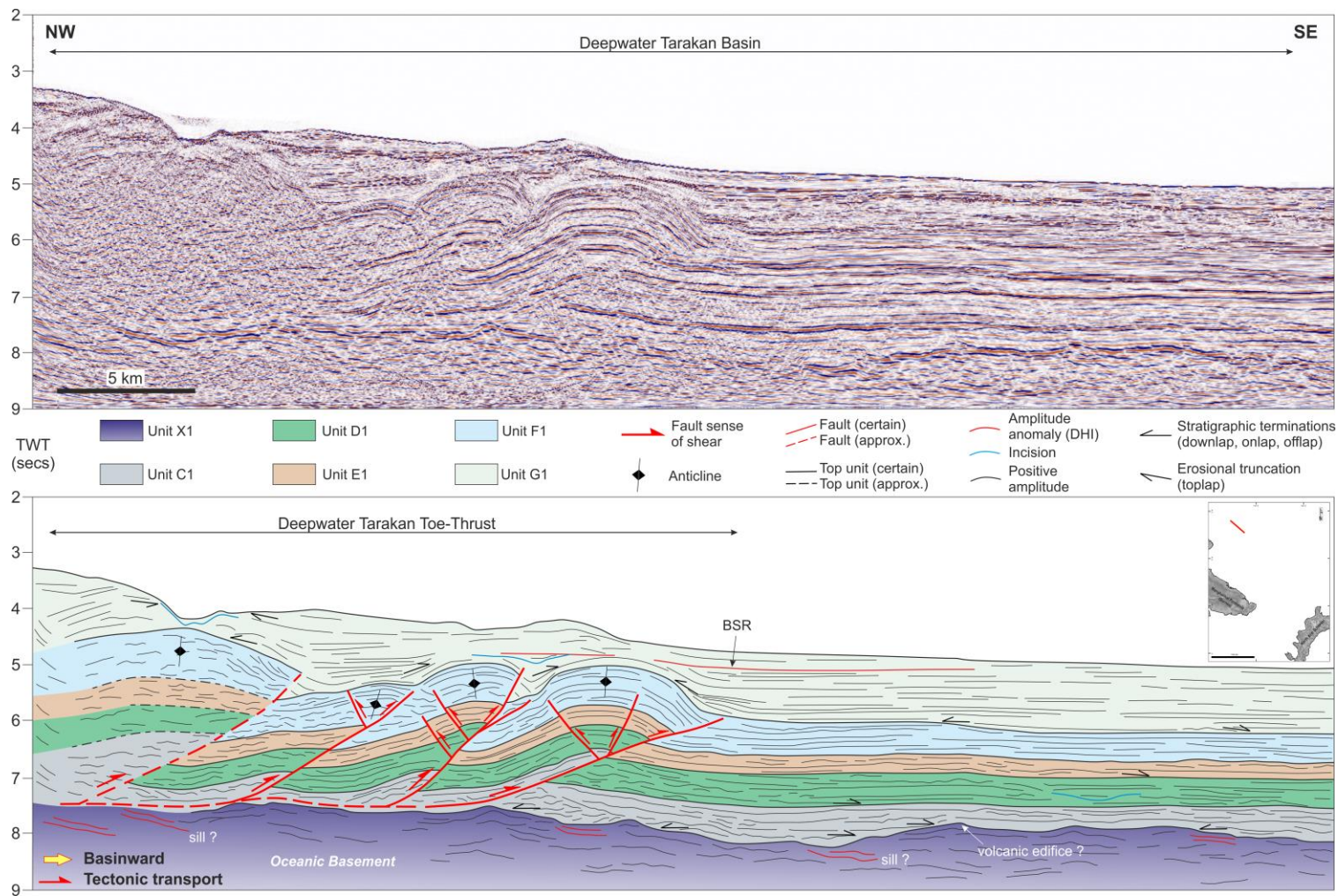
1011 BP, 2000).



1012

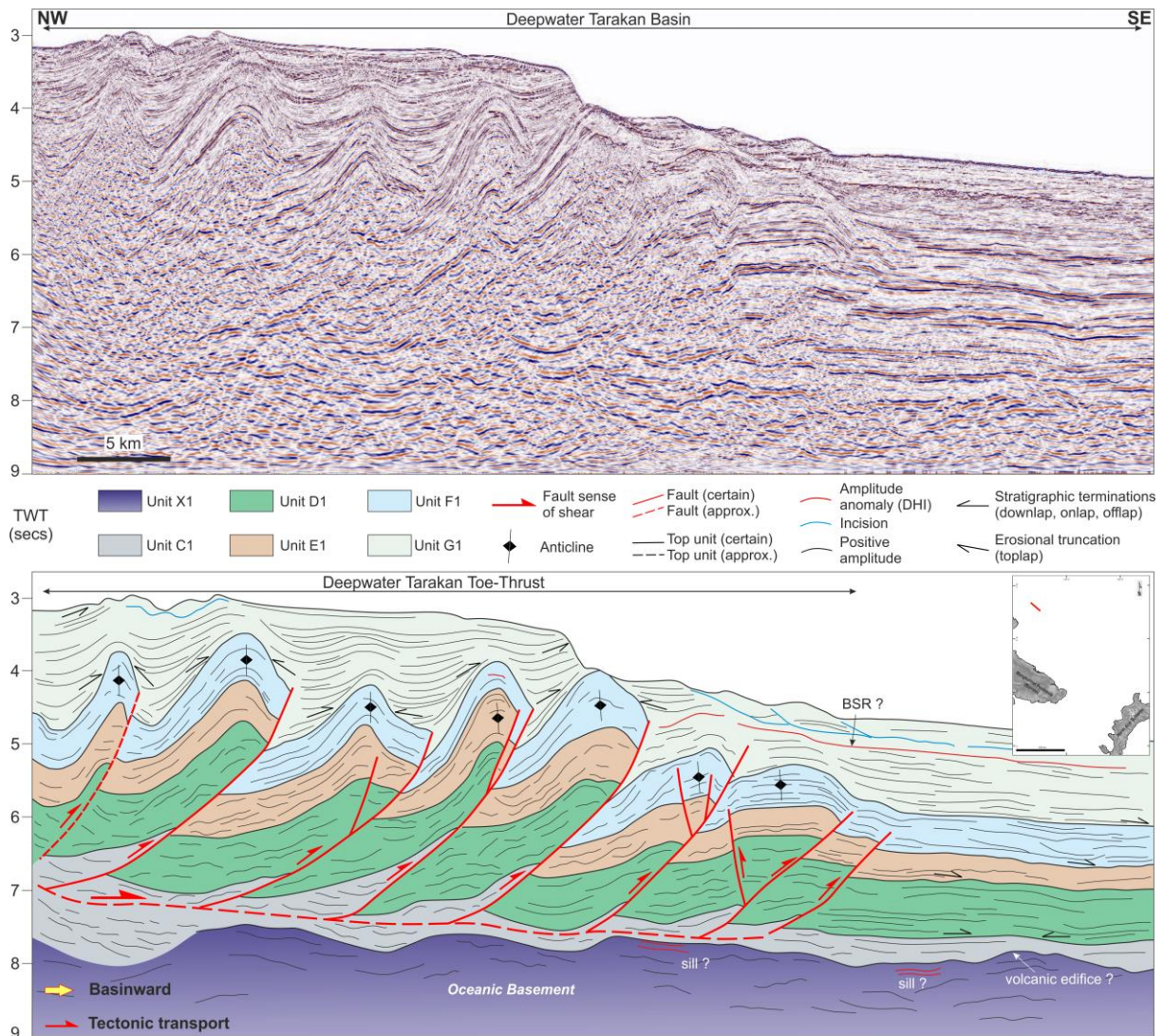
1013 Figure 12. Summarized seismic stratigraphy units of the Deepwater Tarakan Basin modified from various sources (Atzeni and Guritno, 2003; BP, 2000; Haq et al.,

1014 1988; ICS, 2017; PERTAMINA-BPPKA, 1996).



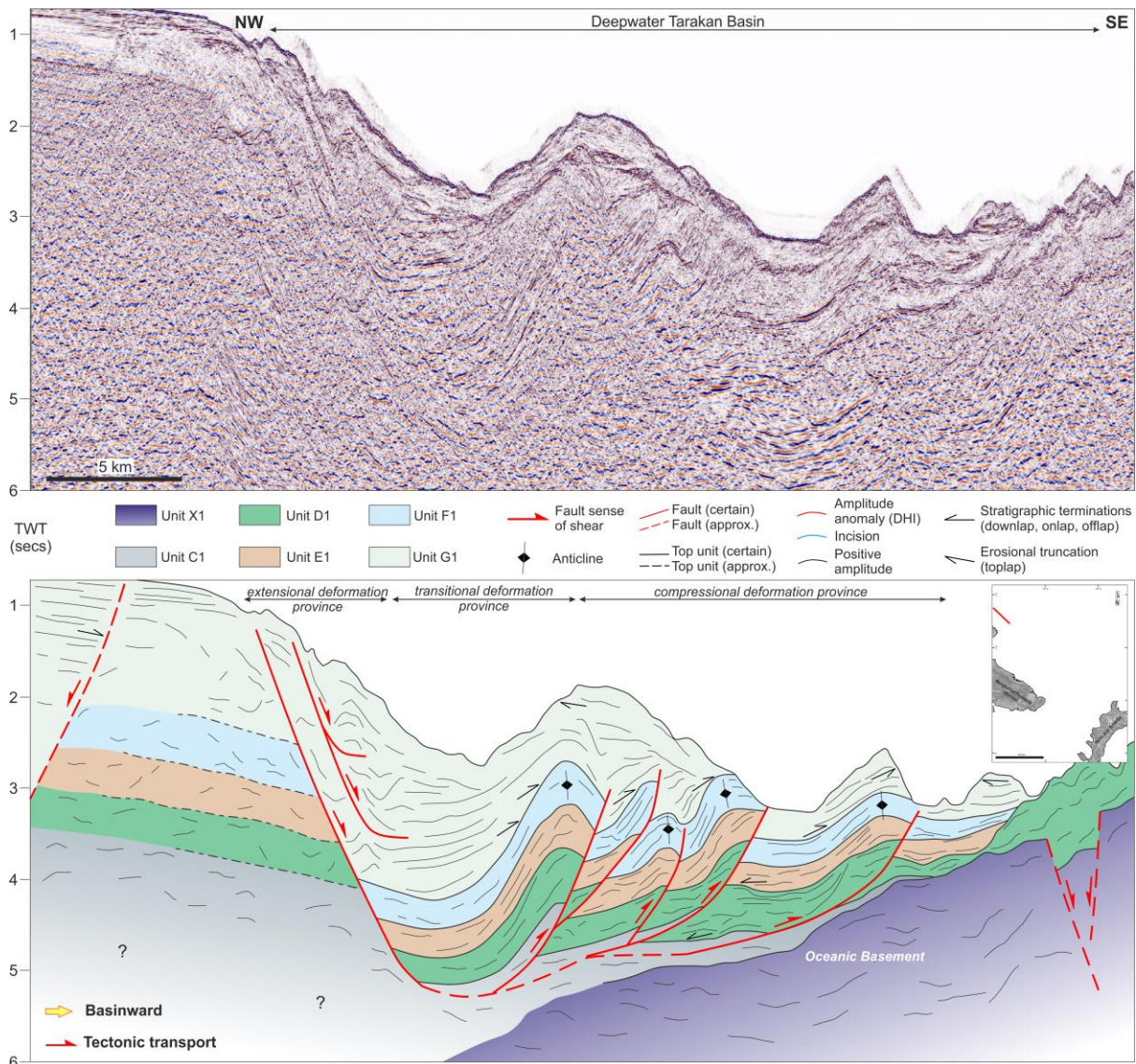
1015

1016 Figure 13. Uninterpreted (above) and interpreted (below) NW-SE seismic section from Deepwater Tarakan Basin exhibit deformed strata in the contractional  
 1017 structural province which formed the Deepwater Tarakan Toe-Thrust and detached within the Unit C1. The toe-thrust deformation younging direction is to the  
 1018 right.



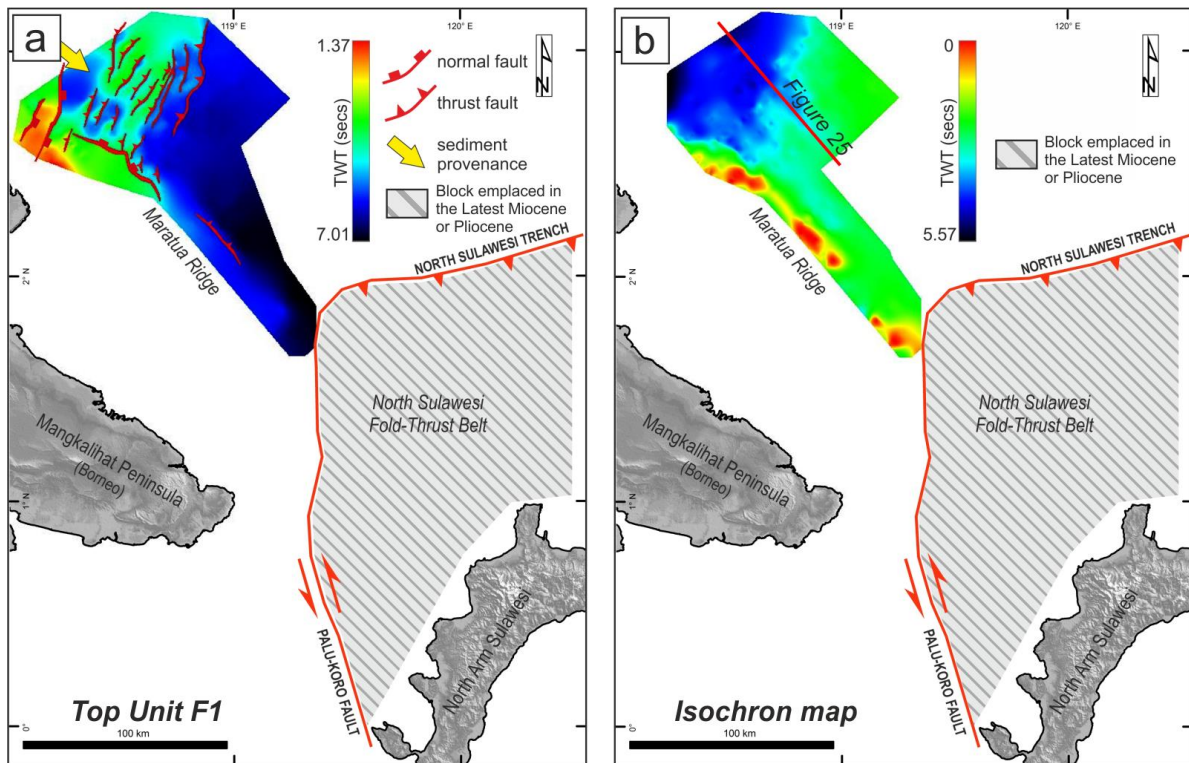
1019

1020 Figure 14. Uninterpreted (above) and interpreted (below) NW-SE seismic section from Deepwater  
 1021 Tarakan Basin showing imbricated styles of fold-thrust belt in the Deepwater Tarakan Toe-Thrust. The  
 1022 toe-thrust deformation younging direction is to the right. Note that younger strata (Unit G1) above pre-  
 1023 kinematic units are not affected much by deformation of fold-thrust belt as growth strata of syn-kinematic  
 1024 and parallel reflection of post-kinematic above, only covered the deformed unit below. Multibeam  
 1025 bathymetry also shows toe-thrust not visible on the seabed (Figure 3).



1026

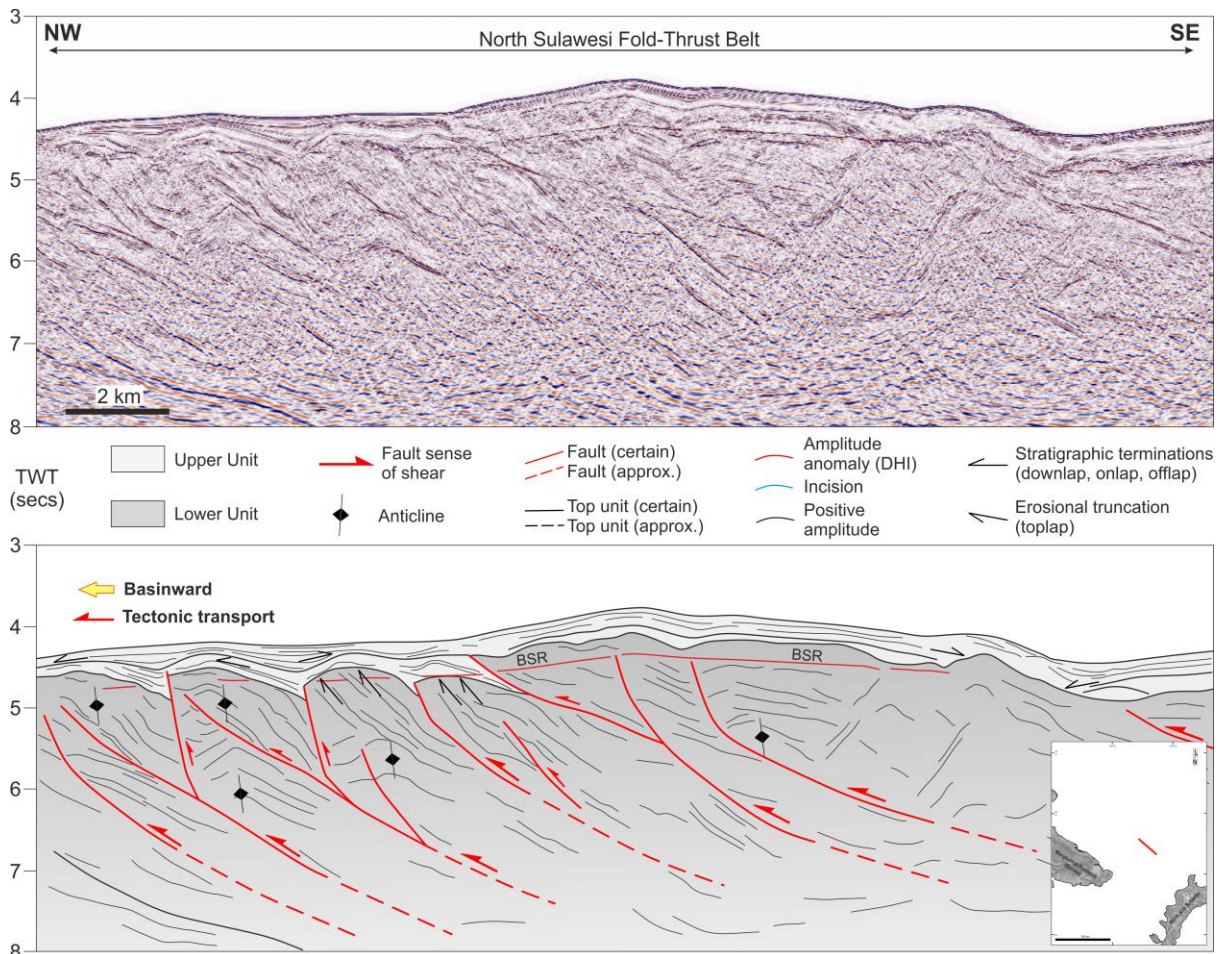
1027 Figure 15. Uninterpreted (above) and interpreted (below) NW-SE seismic section from Deepwater  
 1028 Tarakan Basin exhibit the development of deepwater toe-thrust. The toe-thrust development is driven by  
 1029 gravitational sliding from unstable shelfal area with extensional deformation province that allow large  
 1030 amount of sediment to fall and flow downslope to the basinward. The toe-thrust then developed as  
 1031 compressional deformation province. The toe-thrust deformation younging direction is to the right.  
 1032 Active erosional surface shaped the local incision valley at the seabed as also reflected from multibeam  
 1033 bathymetry shown in Figure 3.



1034

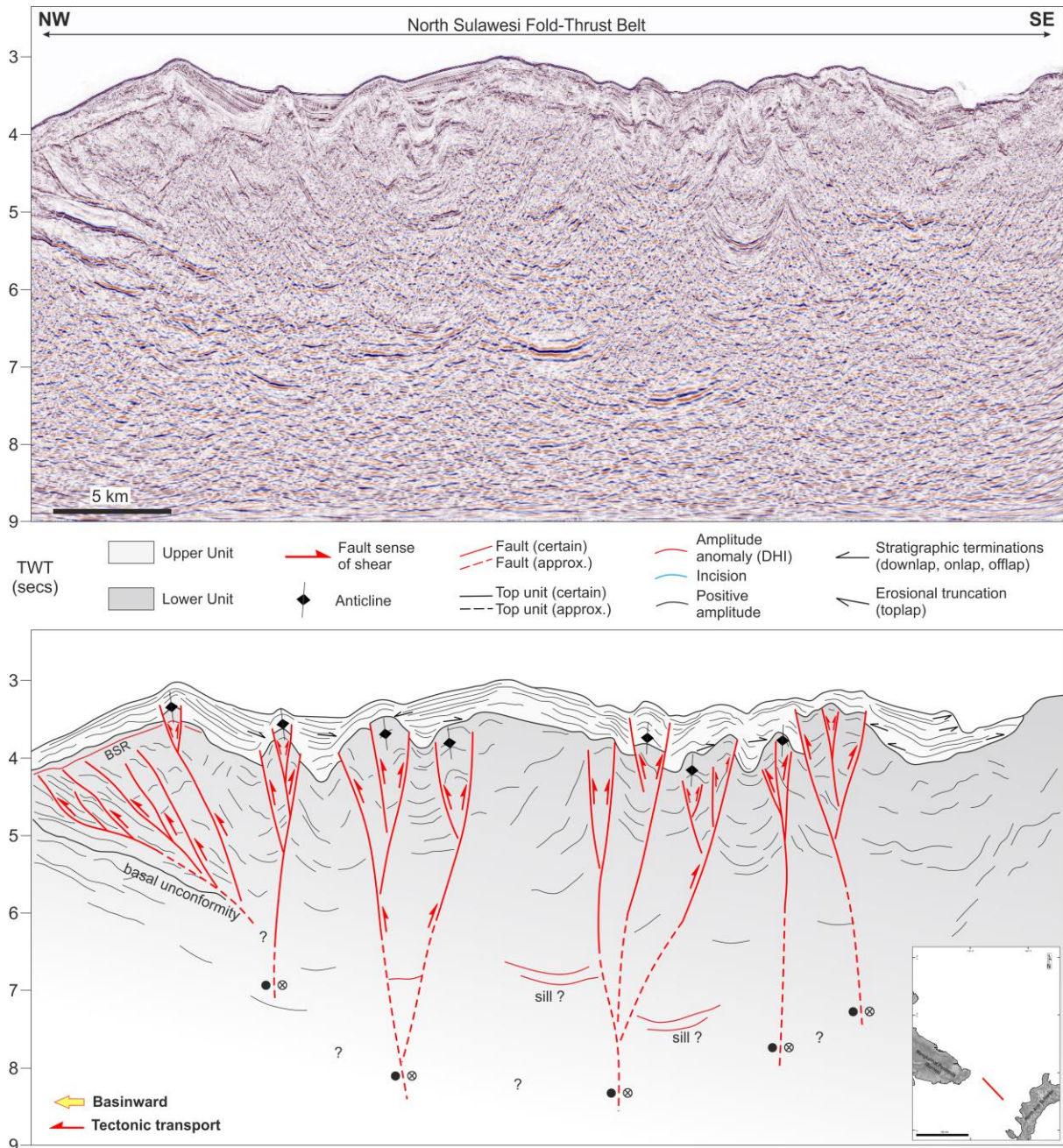
1035 Figure 16. Subsurface map of Deepwater Tarakan Basin. (a) Depth to Top Unit F1 structure map showing  
 1036 the well-developed gravity driven toe-thrust fault. Extensional deformation province is observed in the  
 1037 shallow depth level, whereas compressional deformation province is observed in the toe of the slope. (b)  
 1038 Total sediment thickness map showing great amount of sediment thicknesses were concentrated in the  
 1039 deformed area compare to the distal area to the east.





1040

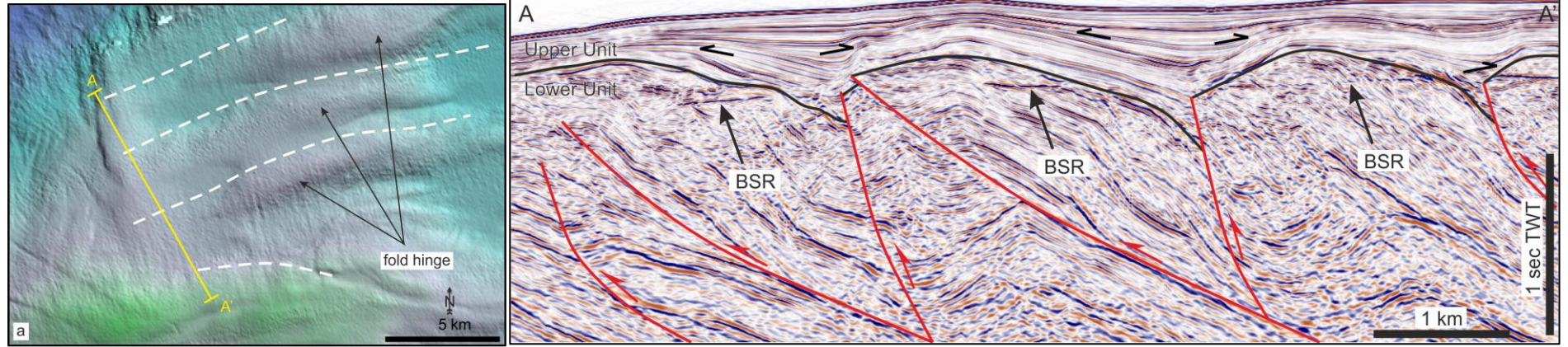
1041 Figure 17. Uninterpreted (above) and interpreted (below) NW-SE seismic section from North Sulawesi  
 1042 Fold-Thrust Belt. The imbricated fold-thrust belt is verging NW, different with tectonic transport of  
 1043 Deepwater Tarakan Toe-Thrust. Also, the seabed expression from seismic and multibeam bathymetry  
 1044 (Figure 3) also showing active deformation of North Sulawesi Fold-Thrust Belt in the present-day. The  
 1045 fold-thrust belt deformation younging direction is to the left.



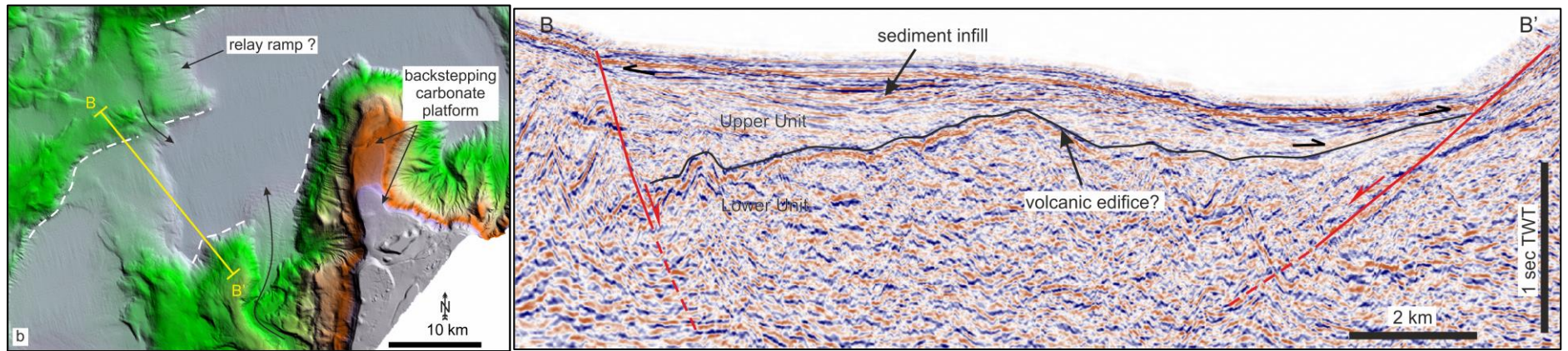
1046

1047 Figure 18. Uninterpreted (above) and interpreted (below) NW-SE seismic section from North Sulawesi  
 1048 Fold-Thrust Belt. The complex Palu-Koro Fault Zone is shown in the left where there are possible  
 1049 underthrusting Eastern Borneo part below the fold-thrust belt. Seismic interpretation also showing  
 1050 several couple shears of Palu-Koro Fault Zone that controlled the morphology and sedimentary  
 1051 architecture of the seabed, indicating active deformation in the present-day.

1052

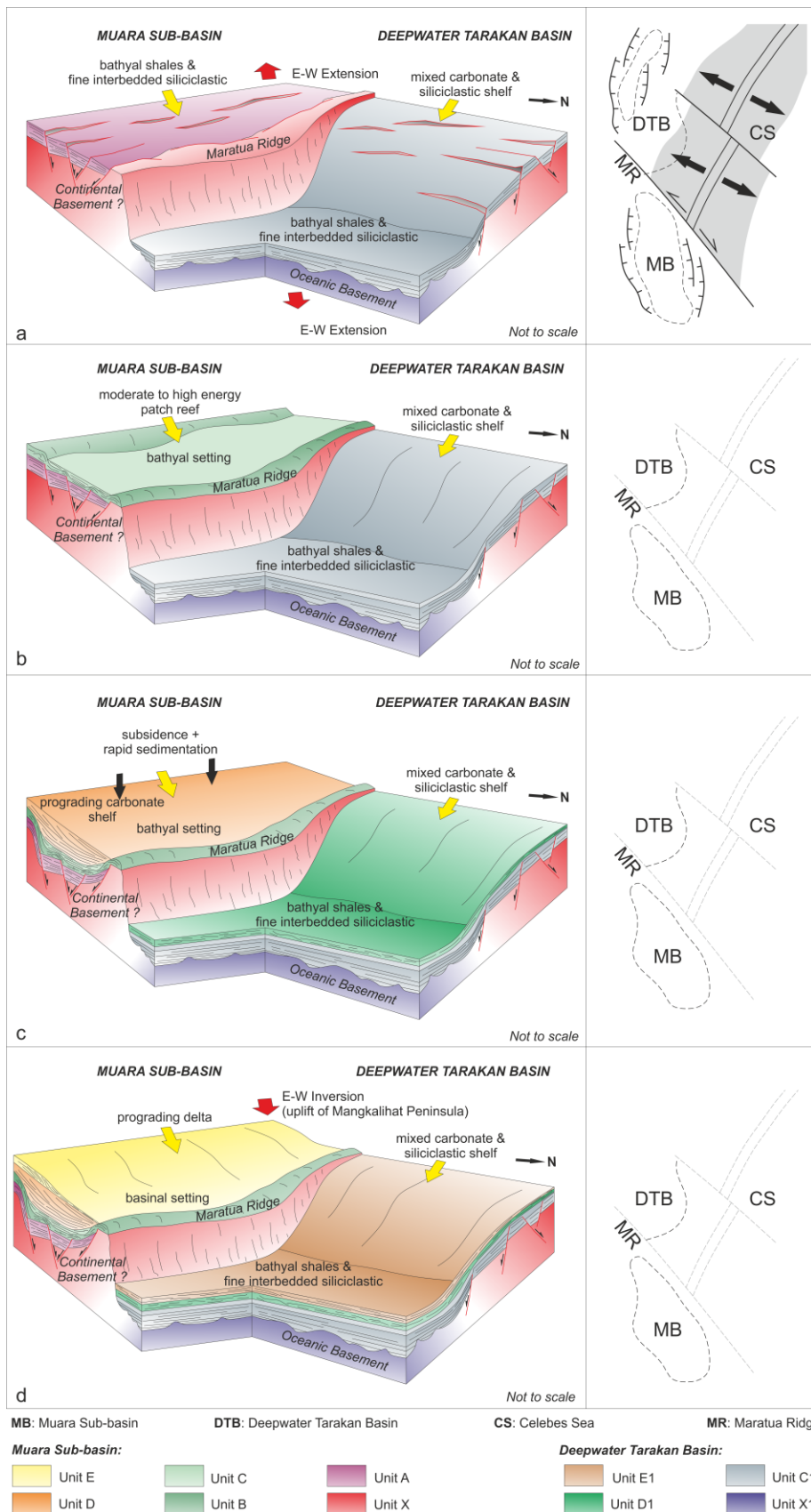


1053



1054 Figure 19. Structural features as observed in the North Sulawesi Fold-Thrust Belt. Illumination direction from NE. (a) Seabed morphology of the fold-thrust belt. (b)

1055 Extensional basin formed in the southern-most part of the North Sulawesi Fold-Thrust Belt. Location is shown in Figure 3.



**Mid-Late Eocene**

Extension began in the Middle Eocene which led to the formation of oceanic crust in the Celebes Sea. Extension is also observed in the Muara Sub-basin.

**Early-Late Oligocene**

The Muara Sub-basin and the adjacent area was mostly covered by widespread carbonate build-up. The Deepwater Tarakan Basin was a deep marine environment. Little sediment was shed to the basinward.

**Early Miocene**

Change of sedimentation character in Borneo. In the Muara Sub-basin, thermal subsidence caused the basin to subside rapidly. Large amount of sediment contributed to the development of an delta system prograding eastward to the Deepwater Tarakan Basin.

**Middle Miocene**

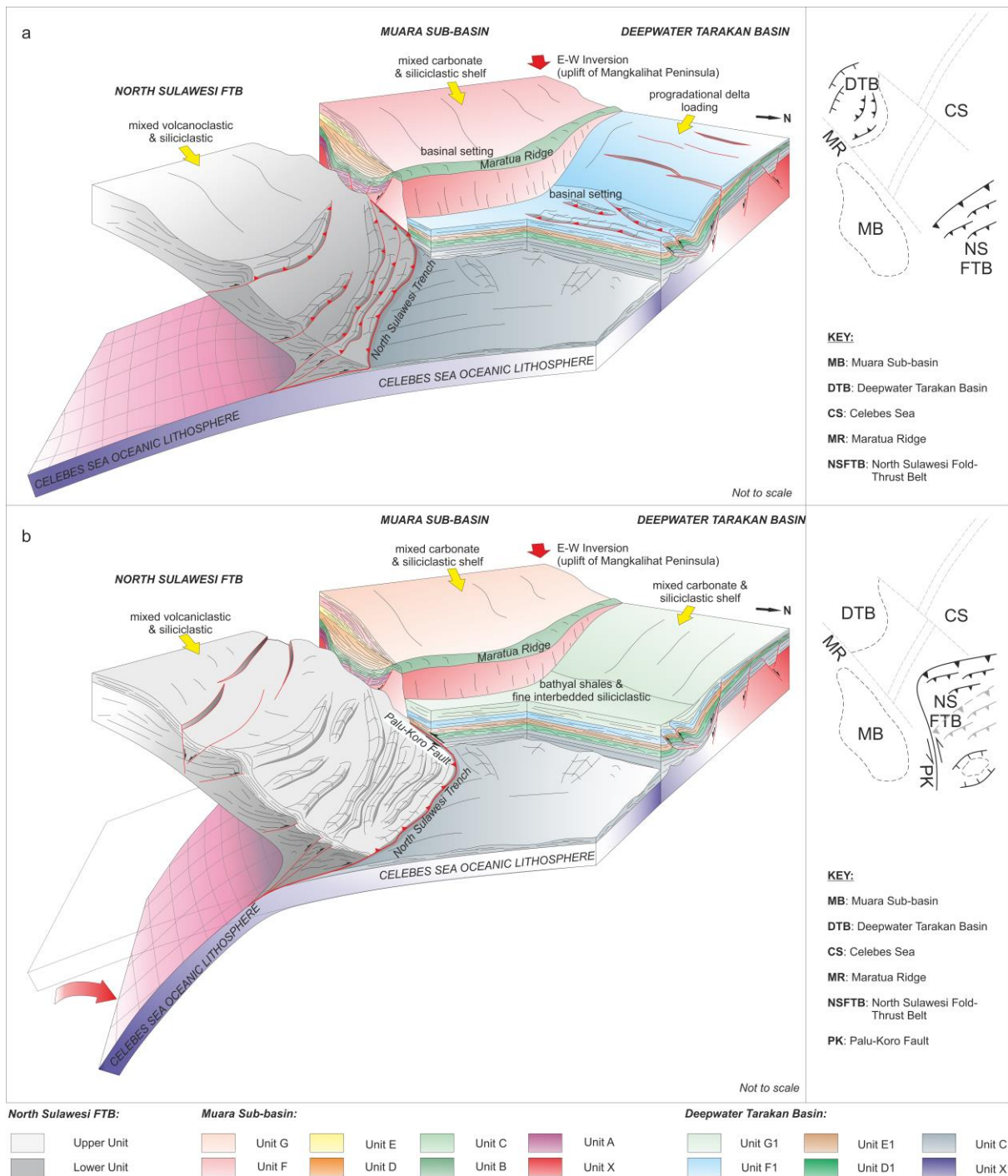
Inversion and uplift caused rapid clastic deltaic deposition in the Tarakan Basin and it seems to have prograded to the basinal area. Inversion and uplift in the Mangkalihat Peninsula and adjacent areas also caused prograding deltaic deposition in the Muara Sub-basin.

1056

1057 Figure 20. Schematic diagram illustrating the structural and stratigraphic evolution model of the Offshore

1058 NW Sulawesi. (a) Middle-Late Eocene stage. (b) Early-Late Oligocene stage. (c) Early Miocene stage. (d)

1059 Middle Miocene stage.



1060

1061

1062

1063

1064

1065

1066

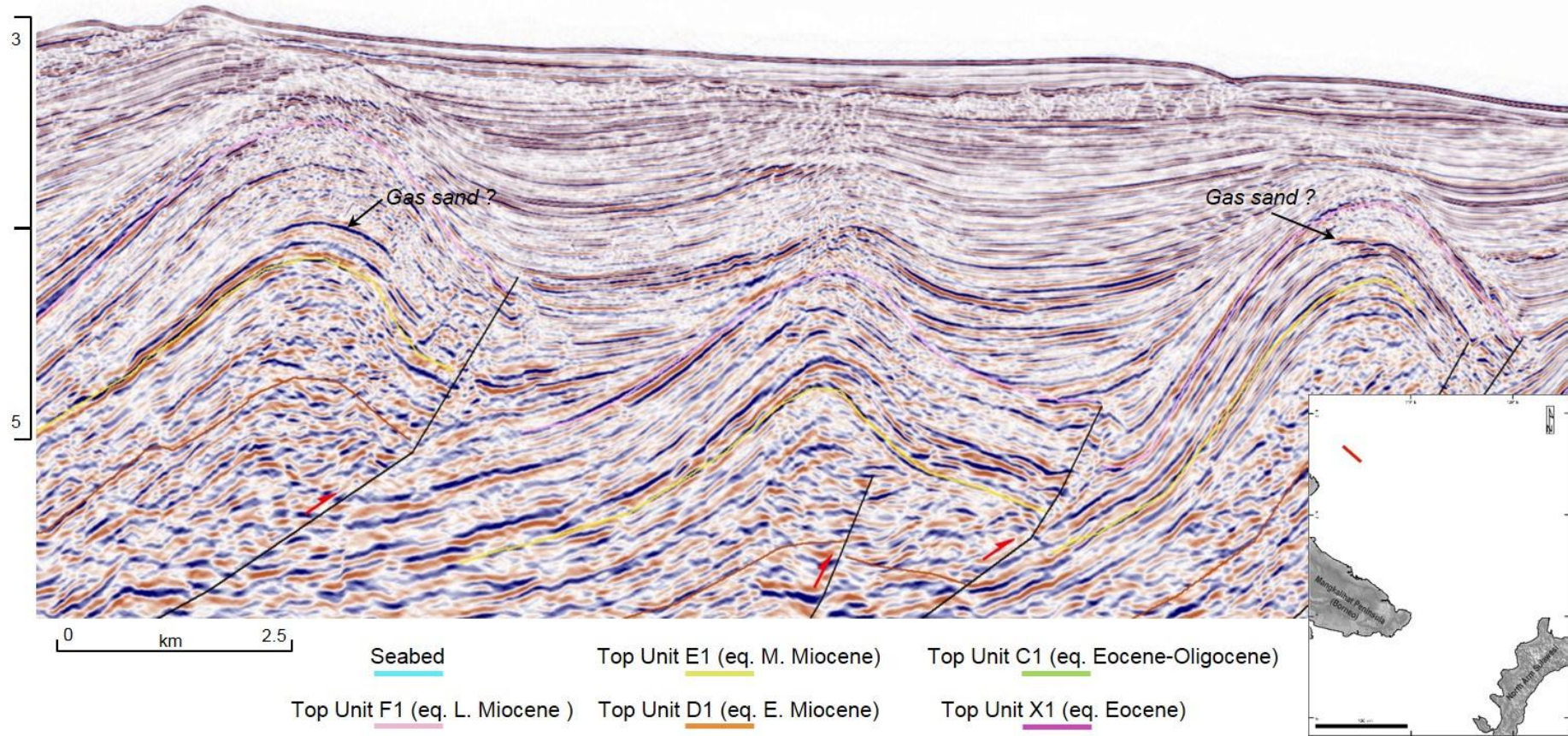
1067

Figure 21. Schematic diagram illustrating the structural and stratigraphic evolution model of the Offshore NW Sulawesi. (a) In the Late Miocene stage, inversion and uplifting seem to have continued caused mixed carbonate and siliciclastic prograded into the Muara Sub-basin. Similarly, in the Deepwater Tarakan Basin, rapid clastic deposition from landward to the basin caused loading of the prograding delta. Consequently, normal faulting in the shelf caused gravity driven movements and formed Deepwater Tarakan Toe-Thrust faults. At the same time, the subducting Celebes Sea is interpreted to have occurred in the Latest Miocene and developed North Sulawesi Fold-Thrust Belt. (b) Inversion and uplift in Borneo are

1068 interpreted to have continued from Middle Miocene until the present-day. This caused progradation of  
1069 the shelf which developed during the Pliocene to present-day in both Muara Sub-basin and Deepwater  
1070 Tarakan Basin. Development of toe-thrust faulting in the Deepwater Tarakan Basin is interpreted as  
1071 inactive since the Pleistocene. Rollback of North Sulawesi Trench has caused clockwise rotation and  
1072 moved towards the north to its present-day position, whereas immediately north of North Arm of  
1073 Sulawesi in the offshore extension and subsidence were well developed, followed by deposition of Upper  
1074 Unit.  
1075

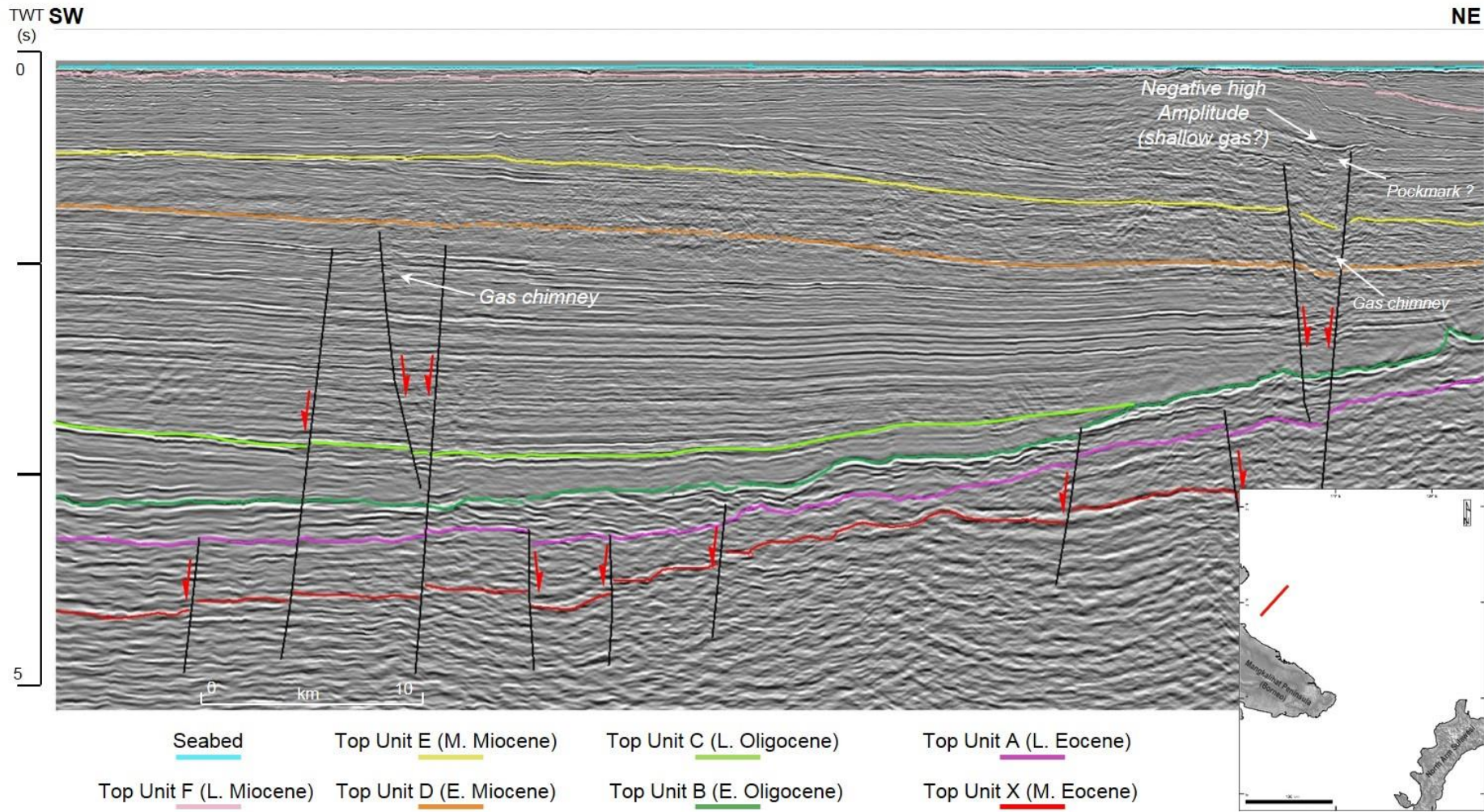
TWT  
(s) NW

SE



1076

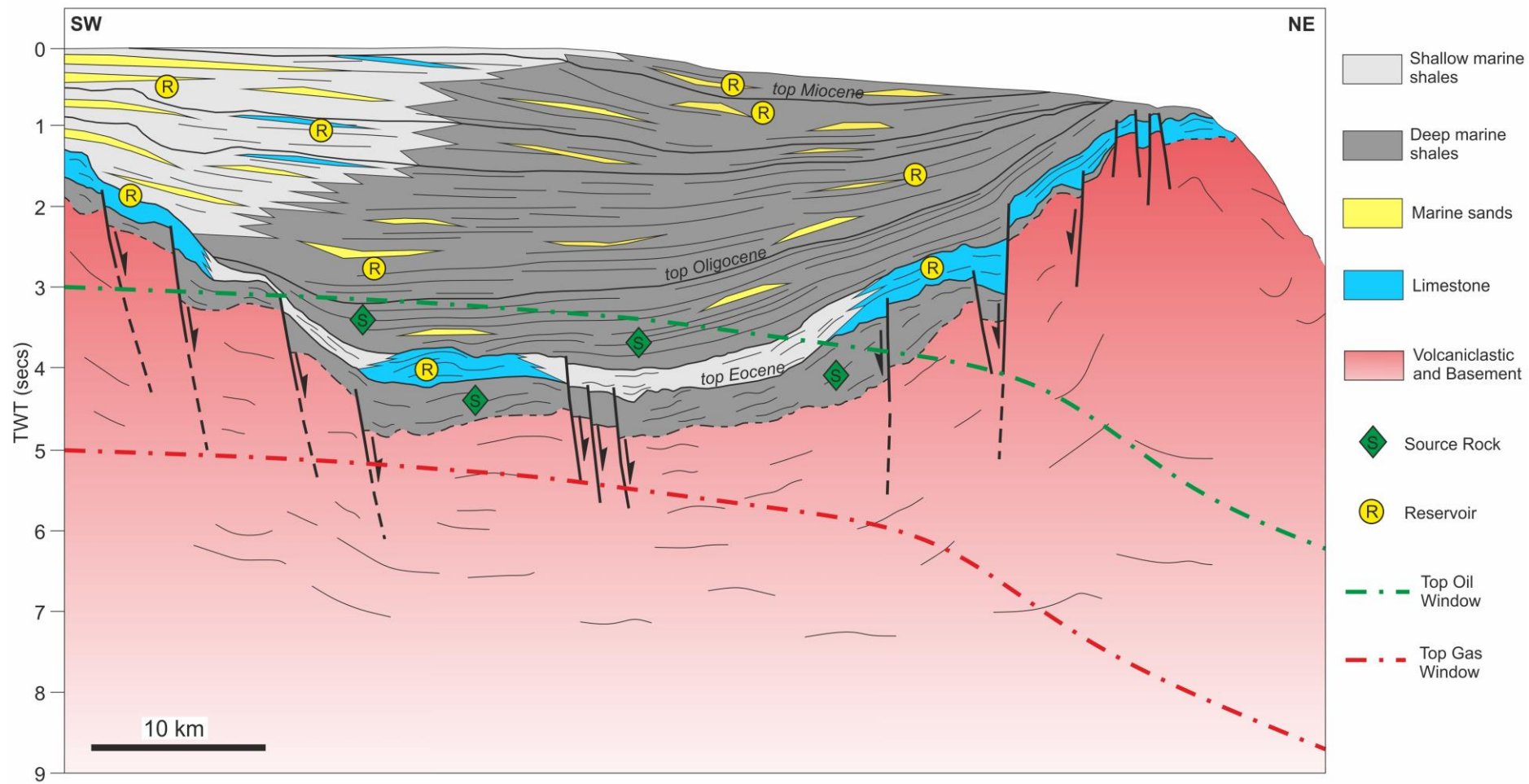
1077 Figure 22. Direct Hydrocarbon Indicators (DHI) indicates potential biogenic gas bearing sand in the Deepwater Tarakan Basin.



1078

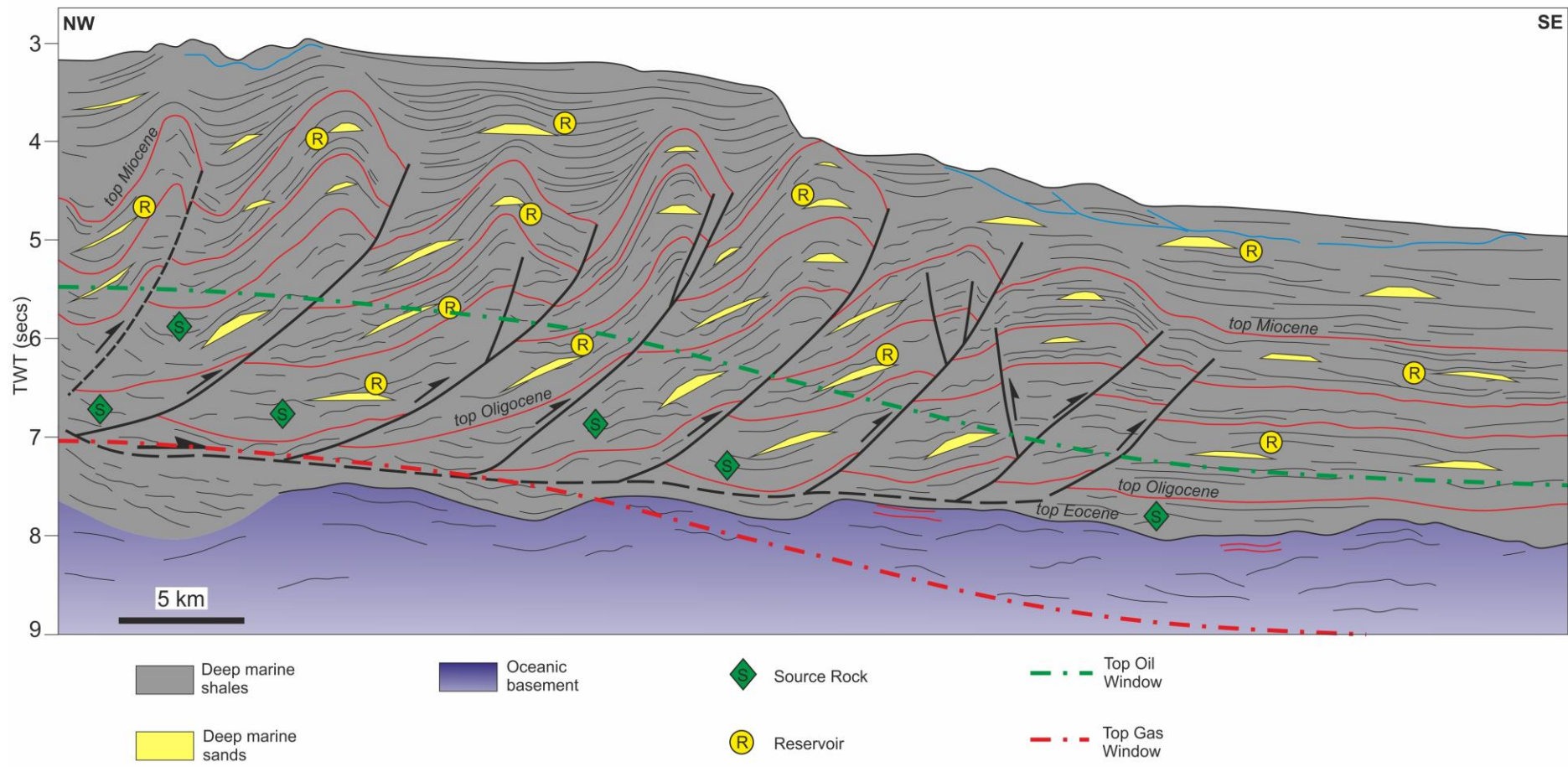
1079 Figure 23. Direct Hydrocarbon Indicators (DHI) indicate gas leakage utilizing normal faults in the Muara Sub-basin.





1080

1081 Figure 24. Schematic cartoon shows play cross-section in the Muara Sub-basin. Location is shown in Figure 10d.



1082

1083 Figure 25. Schematic cartoon shows play cross-section in the Deepwater Tarakan Basin. Location is shown in Figure 16b.